

SOLUTION MANIFOLD AND ITS STATISTICAL APPLICATIONS

BY YEN-CHI CHEN

*Department of Statistics
University of Washington*

FEBRUARY 14, 2020

A solution manifold is the collection of points in a d -dimensional space satisfying a system of s equations with $s < d$. Solution manifolds occur in several statistical problems including hypothesis testing, curved-exponential families, constrained mixture models, partial identifications, and nonparametric set estimation. We analyze solution manifolds both theoretically and algorithmically. In terms of theory, we derive five useful results: the smoothness theorem, the stability theorem (which implies the consistency of a plug-in estimator), the convergence of a gradient flow, the local center manifold theorem and the convergence of the gradient descent algorithm. To numerically approximate a solution manifold, we propose a Monte Carlo gradient descent algorithm. In the case of likelihood inference, we design a manifold constraint maximization procedure to find the maximum likelihood estimator on the manifold. We also develop a method to approximate a posterior distribution defined on a solution manifold.

1. Introduction. In statistics, constructing an estimator or defining a population quantity of interest by solving a system of equation is very common. The maximum likelihood estimator (MLE) is often obtained by solving the score equations (van der Vaart, 1998). The estimating equation defines an estimator by solving a system of equations (Liang and Zeger, 1986). In method of moments approach, an estimator is formed by solving the moment equations (Hansen, 1982). In addition to the above parametric models, solving equations also defines an estimator or a population quantity of interest in a nonparametric setting. In mode hunting problems (Romano, 1988a,b), a necessary condition to a local mode is the gradient being 0 (under smoothness condition). In density level set problem (Tsybakov, 1997), the level set is defined via solving the density-level equation (e.g., $p(x) - \lambda = 0$, where $p(x)$ is the PDF and λ is level of interest).

In most of these examples, the number of parameters d and the number of equations s are the same and the system of equations has to be full rank to obtain a stable estimator. However, there are cases where the number of parameters is larger than the number of equations (i.e., $s < d$), leading to a scenario where the solution contains an infinite number of feasible parameters (under-identified case). While there has been a tremendous amount of literature on the analysis of regular cases ($s = d$), little is known about the behavior when $s < d$. The goal of this paper is to analyze the problem when $s < d$ and design a practical algorithm to find the manifold.

Under smoothness conditions, the feasible set forms a manifold known as a solution manifold (Rheinboldt, 1988). Formally, let $\Psi : \mathbb{R}^d \mapsto \mathbb{R}^s$ be a vector-valued function with $s < d$. The solution set of Ψ

$$M = \{x : \Psi(x) = 0\}$$

MSC 2010 subject classifications: Primary 62F30; secondary 62H05, 65D18

Keywords and phrases: set estimation, gradient descent, manifold, mixture model, nonconvex optimization, constrained likelihood

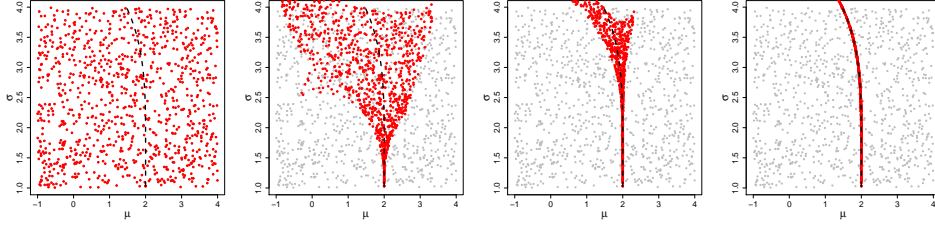


FIG 1. An example of a solution manifold formed by the parameter (μ, σ) of a Gaussian with a tail probability bound $P(-5 < Y < 2) = 0.5$. The left panel shows 1000 random initializations (uniformly distributed within $[1, 3] \times [2, 4]$) and then we keep applying the gradient descent algorithm until convergence (right panel). The black dashed line indicates the actual location of the solution manifold.

is called the solution manifold and we call Ψ the generator function of M . Note that in some applications, x represents the parameter in a model, so sometimes we write $M = \{\theta : \Psi(\theta) = 0\}$. Here we provide some examples of solution manifolds from common statistical problems.

Example 1 (Constrained likelihood space) Consider a parametric model $p(y; \theta)$ where $\theta \in \mathbb{R}^d$ is the parameter vector. Suppose that we have a set of constraints on the model such that

$$f_1(\theta) = f_2(\theta) = \dots = f_s(\theta) = 0$$

for some given functions f_1, \dots, f_s ; these functions may be from independence assumptions or moment constraints $\mathbb{E}(g_j(Y)) = 0$ for some functions g_1, \dots, g_s . It is easy to see that the set of parameters that satisfies these constraints is

$$(1) \quad \Theta_0 = \{\theta : f_\ell(\theta) = 0, \ell = 1, \dots, s\} = \{\theta : \Psi(\theta) = 0\},$$

which is a solution manifold with $\Psi_\ell(\theta) = \int f_\ell(y)p(y; \theta)dy$. The above model occurs in algebraic statistics (Drton and Sullivant, 2007; Michalek et al., 2016), partial identification problems with equality constraints (Hansen, 1982; Chernozhukov et al., 2007) and mixture models with moment constraints (Lindsay, 1995; Chauveau and Hunter, 2013). We will return to this problem in Section 4.1.2 and 4.2. Figure 1 shows an example of a solution manifold formed by the tail probability constraint $P(-5 < Y < 2) = 0.5$ where $Y \sim N(\mu, \sigma^2)$. There are two parameters (μ, σ^2) and one constraint so the resulting solution set is a 1-dimensional manifold. From the left to the right panels, we show that by random initializations with a suitable gradient descent process (Algorithm 1), we are able to recover the underlying manifold.

Example 2 (Curved exponential family) Suppose that we are interested in a set of parameters $\theta \in \mathbb{R}^d$ and they are associated with the generated data via a parametric model from the exponential family with model parameter $\eta(\theta) \in \mathbb{R}^s$ such that

$$p(y; \theta) \propto \exp(T(y)^T \eta(\theta)),$$

where $T(y) = (T_1(y), \dots, T_s(y))^T$ is the sufficient statistics. When $d < s$, this is the usual curved exponential family (Efron, 1975, 1978). When $d > s$, this is an unidentified model but we can still view it as a solution manifold. Within this model, we can only identify η (using a traditional method such as the MLE) and let η_0 be the best fit to the data. This implies that we can only identify θ as the set

$$\{\theta : \eta(\theta) - \eta_0 = 0\} \subset \mathbb{R}^d,$$

which is a solution manifold with $\Psi(\theta) = \eta(\theta) - \eta_0$. More details about this example will be provided in Section 4.1.3.

Example 3 (Under-constrained Z-estimator) For a parameter of interest $\theta \in \mathbb{R}^d$, an Z-estimator (van der Vaart, 1998) is the solution to the estimating equation

$$\hat{\theta} : \frac{1}{n} \sum_{i=1}^n Z(Y_i; \hat{\theta}) = 0$$

where $Z(y; \theta) \in \mathbb{R}^d$ and Y_1, \dots, Y_n are IID random variables from some distribution. A population version of the Z-estimator is

$$\theta_0 : \mathbb{E}(Z(Y; \theta_0)) = 0.$$

When we have less estimating equations than the number of parameters, we have several solutions that solve $\mathbb{E}(Z(Y; \theta)) = 0$ and the collection of these solutions form a solution manifold. In a sense, one can view the solution manifold as a generalized Z-estimator. The under-constrained Z-estimator occurs in causal inference, where we would like to use an instrumental variable approach to analyze the causal effect. If the number of the instrument is less than the number of endogenous variables, we ran in to this problem; see Example 4 of Chernozhukov et al. (2007) for more details.

Example 4 (Density ridges) A k -ridge (Genovese et al., 2014) of a density function $p(x)$ is defined as the collection of points satisfying

$$\{x : V_k(x)^T \nabla p(x) = 0, \lambda_k(x) < 0\},$$

where $V_k(x) = [v_k(x), \dots, v_d(x)] \in \mathbb{R}^{(k-d)}$ are the collection of eigenvectors of $H(x)$ and $\lambda_k(x)$ is the k -th eigenvector and the eigen-pairs are ordered as $\lambda_1(x) \geq \lambda_2(x) \geq \dots \geq \lambda_d(x)$. In this case $\Psi(x) = V_k(x)^T \nabla p(x)$ so ridges are also solution manifolds. In addition to ridges, level sets and critical points of a function (Walther, 1997; Mammen and Polonik, 2013; Chacón, 2015) are exampls of solution manifolds. We will discuss this in Section 4.4

Main results. Our main results include theoretical developments and algorithmic innovations. In the theoretical analysis, we show that under the same assumptions (F1-2), we have the followings:

1. **Smoothness theorem.** The solution manifold is a $(d - s)$ -dimensional manifold with a positive reach (Lemma 1 and Theorem 3).
2. **Stability theorem.** As long as $\hat{\Psi}$ and Ψ and their derivatives are sufficiently close, $\widehat{M} = \{x : \hat{\Psi}(x) = 0\}$ converges to M under the Hausdorff distance (Theorem 4).
3. **Convergence of a gradient flow.** For the gradient descent flow of $\|\Psi(x)\|^2$, the flow converges (in the normal direction of M) to a point on M when the starting point is sufficiently close to M (Theorem 6).
4. **Local center manifold theorem.** The collection of points converging to the same location $z \in M$ forms an s -dimensional manifold (Theorem 7).
5. **Convergence of a gradient descent algorithm.** With a good initialization, the gradient descent algorithm of $\|\Psi(x)\|^2$ converges linearly to a point in M (Theorem 8) when the step size is sufficiently small.

To numerically find solution manifolds and use them for handling statistical problems, we propose three algorithms:

1. **Monte Carlo gradient descent algorithm:** an algorithm generating points over M that requires only the access to Ψ and its gradient (Section 3 and Algorithm 1).

2. **Manifold-constraint maximizing algorithm:** an algorithm that finds the MLE on the solution manifold (Section 4.1.1 and Algorithm 2).
3. **Approximated manifold posterior algorithm:** a Bayesian procedure that approximates the posterior distribution on a manifold (Section 4.3 and Algorithm 3).

The impact of this paper is beyond statistics. Our result provides a new analysis of the partial identification problem in econometrics (Hansen, 1982; Chernozhukov et al., 2007). The local center manifold theorem offers a new class of statistical problems where the dynamical system interacts with statistics (Perko, 2001). The Monte Carlo approximation of a solution manifold leads to a point cloud over the manifold, which is a common scenario in computational geometry (Cheng et al., 2005b,a; Dey, 2006). The algorithmic convergence of the gradient descent demonstrates a new class of non-convex functions that we still obtain the linear convergence (Boyd and Vandenberghe, 2004; Nesterov, 2018).

Outline. The paper is organized as follows. In Section 2, we provide a formal definition of a solution manifold and study the smoothness and stability of the manifold. In Section 3, we propose an algorithm for approximating the solution manifold and analyze its properties. In Section 4, we discuss several statistical applications of solution manifolds and propose algorithms for optimization and Bayesian inference. In Section 5, we discuss future directions, connections with other fields, and some manifolds in statistics that are not in a solution form.

Notations. Let $v \in \mathbb{R}^d$ be a vector and $V \in \mathbb{R}^{n \times m}$ be a matrix. $\|v\|_2$ is the L_2 norm (Euclidean norm) of v and $\|v\|_{\max} = \max\{\|v_1\|, \dots, \|v_d\|\}$ is the vector max norm. For matrices, we use $\|V\| = \|V\|_2 = \max_{\|u\|=1, u \in \mathbb{R}^m} \frac{\|Vu\|_2}{\|u\|_2}$ as the L_2 norm and $\|V\|_{\max} = \max_{i,j} \|V_{ij}\|$ as the max norm. For a squared matrix A , we define $\lambda_{\min}(A)$, $\lambda_{\max}(A)$ to be the minimal and maximal eigenvalue and $\lambda_{\min, > 0}^2(A)$ to be the smallest non-zero eigenvalue. For a vector value function Ψ , we define a maximal norm of derivatives as

$$\|\Psi\|_{\infty}^{(J)} = \sup_x \max_i \max_{j_1} \dots \max_{j_J} \left| \frac{\partial^J}{\partial x_{j_1} \dots \partial x_{j_J}} \Psi_i(x) \right|$$

for $J = 0, 1, 2, 3$. When Ψ is a scalar function, this reduces to

$$\|\Psi\|_{\infty}^{(1)} = \sup_x \|\nabla \Psi(x)\|_{\max}, \quad \|\Psi\|_{\infty}^{(2)} = \sup_x \|\nabla \nabla \Psi(x)\|_{\max}$$

are the usual maximal norm of the gradient vector and Hessian matrix over all x . We also define

$$\|\Psi\|_{\infty, J}^* = \max_{j=0, \dots, J} \|\Psi\|_{\infty}^{(j)}$$

as a norm that measures distance using upto the J -th derivative. The gradient of $\Psi(x)$ is an $s \times d$ matrix

$$G_{\Psi}(x) = \nabla \Psi(x) = \begin{bmatrix} \nabla \Psi_1(x)^T \\ \nabla \Psi_2(x)^T \\ \dots \\ \nabla \Psi_s(x)^T \end{bmatrix} \in \mathbb{R}^{s \times d}$$

and the Hessian of $\Psi(x)$ will be an $s \times d \times d$ array

$$H_{\Psi}(x) = \nabla \nabla \Psi(x) \in \mathbb{R}^{s \times d \times d}, \quad [H_{\Psi}(x)]_{ijk} = \frac{\partial^2}{\partial x_j \partial x_k} \Psi_i(x)$$

and third derivative of Ψ will be an array

$$\nabla\nabla\nabla\Psi(x) \in \mathbb{R}^{s \times d \times d \times d}, \quad [\nabla\nabla\nabla\Psi(x)]_{ijkl} = \frac{\partial^3}{\partial x_j \partial x_k \partial x_\ell} \Psi_i(x).$$

Let A be a set and x be a point, we define

$$d(x, A) = \inf\{\|x - y\| : y \in A\}$$

as the projected distance from x to A .

2. Solution manifold and its geometry. Let $\Psi : \mathbb{R}^d \mapsto \mathbb{R}^s$ be a vector-valued function and let $M = \{x : \Psi(x) = 0\}$ be the solution set/manifold. When the gradient matrix $G_\Psi(x) = \nabla\Psi(x)$ has rank s at every $x \in M$, the set M is an s -dimensional manifold locally at every point x due to the implicit function theorem (Rudin, 1964). In algebraic statistics, parameters in the solution set $\{x : \Psi(x) = 0\}$ is called an implicit (statistical) algebraic model (Gibilisco et al., 2010).

For a solution manifold, its normal space can be characterized using the following lemma.

Lemma 1 *For every point $x \in M$, the row space of $G_\Psi(x) \in \mathbb{R}^{s \times d}$ spans the normal space of M at x .*

Namely, the gradient of each function Ψ_ℓ is normal to the solution manifold. This is a natural result since the gradient of a function is always normal to the level set and the solution manifold can be viewed as the intersection of level sets of different functions.

2.1. Assumptions. In this paper, we will make the following two major assumptions. As we will show in this paper, all the theoretical results rely on these two assumptions.

(F1) $\Psi(x)$ is bounded three-times differentiable and $\|\Psi\|_{\infty,3}^* < \infty$.

(F2) There exists $\lambda_0, \delta_0, c_0 > 0$, such that

1. $\lambda_{\min}(G_\Psi(x)G_\Psi(x)^T) \equiv \lambda_{\min,>0}(G_\Psi(x)^T G_\Psi(x)) > \lambda_0^2$ for all $x \in M \oplus \delta_0$ and
2. $\|\Psi(x)\|_{\max} > c_0$ for all $x \notin M \oplus \delta_0$.

Assumption (F1) is an ordinary smoothness of the generator function. It may be relaxed by a Hölder type condition on $\Psi(x)$ that requires the existence and smoothness of the second derivative of $\Psi(x)$. In fact, some theoretical results require weaker assumptions than (F1) and we provide more discussions about this in Section 5.1. Assumption (F2) is a curvature assumption of Ψ around the solution manifold. By Lemma 1, it implies that the normal space of M at each point is well-defined. This assumption will reduce to some commonly assumed conditions in the literature. For instance, in the case of mode estimation (finding the local modes of a PDF $p(x)$), (F2) reduces to the assumption that the local modes are well-defined as separated (Romano, 1988a,b). This is similar to the assumption that the PDF $p(x)$ is a Morse function (Chen et al., 2016; Jisu et al., 2016). In the MLE theory, (F2) means that Fisher's information matrix is positive definite at the MLE (and other local maxima). In the problem of finding the density level sets (finding the set $\{x : p(x) = \lambda\}$), this assumption is equivalent to assuming that $p(x)$ has non-zero gradient around the level set (Molchanov, 1991; Tsybakov, 1997; Molchanov, 1998; Cadre, 2006; Mammen and Polonik, 2013; Laloe and Servien, 2013).

The constants in (F2) can be further characterized by the following lemma.

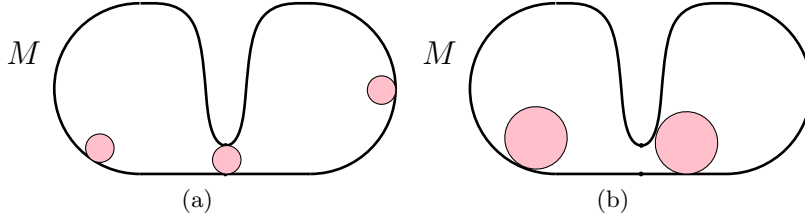


FIG 2. An illustration for reach. Reach is the largest radius for a ball that can freely move along the manifold M without penetrating any part of M . In (a), the radius of the pink ball is the same to the reach. In (b), the radius is too large so that it cannot pass the small gap on M .

Lemma 2 Assume (F1) and that there exists $\lambda_M > 0$ such that

$$\inf_{x \in M} \lambda_{\min}(G_{\Psi}(x)G_{\Psi}(x)^T) \geq \lambda_M^2.$$

Then the constants in (F2) can be chosen as

$$\lambda_0 = \frac{1}{2}\lambda_M, \quad c_0 = \inf_{x \notin M \oplus \delta_0} \|\Psi\|_{\max}, \quad \delta_0 = \frac{3\lambda_M^2}{8\|\Psi_{\infty,1}^*\|\|\Psi_{\infty,2}^*\|}.$$

Lemma 2 only places assumptions on the behavior of Ψ and its derivatives on the manifold M . (F2-1) is the eigengap conditions for the row space of $G_{\Psi}(x)$. The assumption in Lemma 2 is very mild. In the case of estimating local modes of a function, the assumption is the same as requiring the Hessian matrix at local modes have all eigenvalues being positive. The requirement $\inf_{x \in M} \lambda_{\min}(G_{\Psi}(x)G_{\Psi}(x)^T) \geq \lambda_M^2$ implies that rows of $G_{\Psi}(x)$ are linearly independent for all x . Therefore, under (F2-1), the implicit function theorem implies that every point $x \in M$ is locally a $(d-s)$ -dimensional manifold. Assumption (F2-1) only places conditions of Ψ on M while assumption (F2) regularizes the behavior of Ψ in a neighborhood of M . Thus, (F2-1) is a weaker assumption than (F2).

2.2. Smoothness of Solution Manifolds. To describe the smoothness of a manifold, we introduce the concept of *reach* (Federer, 1959; Cuevas, 2009) (also known as condition number in Niyogi et al. 2008 and minimal feature size in Chazal and Lieutier 2005). The reach is the longest distance away from M that every point within this distance to M has a unique projection onto M . i.e.

$$(2) \quad \text{reach}(M) = \inf\{r > 0 : \forall x \in M \oplus r, x \text{ has a unique projection onto } M\},$$

where $M \oplus r = \{x : d(x, M) \leq r\}$. The reach can be viewed as the largest radius of a ball that can freely move along the manifold M ; see figure 2 for an example. The reach has been used in nonparametric set estimation as a condition to guarantee the stability of a set estimator (Chen et al., 2015, 2017; Cuevas, 2009).

The smoothness of Ψ does not suffice to guarantee the smoothness of a solution manifold. Consider the example of a density level set $\{x : p(x) = \lambda\}$ with a smooth density $p(x)$. By construction, this level set is a solution manifold with $\Psi(x) = p(x) - \lambda$, a smooth function. Suppose that $p(x)$ has two modes and a saddle point c . If we choose $\lambda = p(c)$, the level set does not have a positive reach. See Figure 3 for an example.

Although the smoothness of Ψ is not enough to guarantee a smooth M , with an additional condition (F2), the solution manifold will be a smooth one as described in the following theorem.

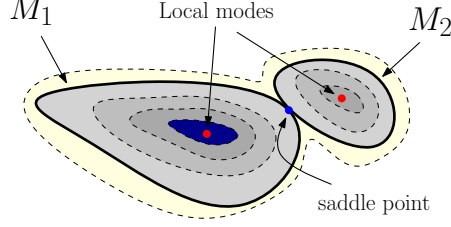


FIG 3. An example of a smooth generator Ψ but the resulting solution manifold $M = M_1 \cup M_2$ may have 0 reach. The dashed line is the contour lines for different levels.

Theorem 3 (Smoothness Theorem) Conditions (F1–2) implies that the reach of M has lower bound

$$\text{reach}(M) \geq \min \left\{ \frac{\delta_0}{2}, \frac{\lambda_0}{\|\Psi\|_{\infty,2}^*} \right\}.$$

Theorem 3 shows a lower bound on the reach of a solution manifold. Essentially, it shows that as long as the generator function is not flat around the solution manifold, the resulting manifold will be smooth. Note that although (F1) requires the existence (and boundedness) of the third derivative of Ψ , Theorem 3 only involves the boundedness of the second derivative. In fact, the reach only requires a β -Hölder with $\beta \geq 2$ and the quantity $\|\Psi\|_{\infty,2}^*$ can be replaced by the Hölder's constant.

Remark 1 Reach is related to the curvature and a quantity called folding (Rice, 1967). The folding is defined as the smallest radius r such that $B(x, r) \cap M$ is connected for each $x \in M$. The first quantity $\frac{\delta_0}{2}$ is related to the folding and the second quantity $\frac{\lambda_0}{K}$ is related to the curvature. When $s = 1$, a similar result to Theorem 3 appears in Walther (1997). Note that the reach is also related to the ‘rolling properties’ and ‘ α -convexity’; see Cuevas (2009) and appendix A of Pateiro López (2008).

2.3. *Stability of Solution Manifolds.* In this section, we show that as two generator functions are sufficiently close, the associated solution manifolds will be similar as well. To measure the distance between two solution manifolds, we use the Hausdorff distance. The *Hausdorff distance* is defined as

$$\text{Haus}(A, B) = \max \left\{ \sup_{x \in B} d(x, A), \sup_{x \in A} d(x, B) \right\}.$$

The Hausdorff distance is a distance between two sets and can be viewed as an L_∞ type distance between sets.

Theorem 4 (Stability Theorem) Let $\Psi, \tilde{\Psi} : \mathbb{R}^d \mapsto \mathbb{R}^s$ be two vector-valued functions and let

$$M = \{x : \Psi(x) = 0\}, \quad \tilde{M} = \{x : \tilde{\Psi}(x) = 0\}$$

be the corresponding solution manifolds. Assume Ψ satisfies (F1–F2) and $\tilde{\Psi}$ is bounded two-times differentiable. When $\|\tilde{\Psi} - \Psi\|_{\infty,2}^*$ is sufficiently small,

1. (F2) holds for $\tilde{\Psi}$.
2. $\text{Haus}(M, \tilde{M}) = O\left(\|\tilde{\Psi} - \Psi\|_{\infty}^{(0)}\right)$.

$$3. \text{ reach}(\widetilde{M}) \geq \min \left\{ \frac{\delta_0}{2}, \frac{\lambda_0}{\|\Psi\|_{\infty,2}^*} \right\} + O \left(\|\widetilde{\Psi} - \Psi\|_{\infty,2}^* \right).$$

Theorem 4 shows that two similar generator functions have similar solution manifolds. Claim 2 is a geometric convergence property that implies that a consistent generator function estimator implies a consistent manifold estimator. Claim 3 is the convergence in smoothness, which implies that \widetilde{M} cannot be too wiggly as $\widetilde{\Psi}$ is sufficiently closed to Ψ .

Similar to the Smoothness Theorem (Theorem 3), we can relax (F1) by assuming only the existence (and boundedness) of the second derivative. We can even relax (F1) by a β -Hölder with $\beta > 2$. Unlike the Smoothness Theorem, here we need the existence of the second derivative so that we can associate the reach of \widetilde{M} to the reach of M .

Example 5 (Curved exponential family) *The stability theorem (Theorem 4) provides a simple approach to obtain the convergence rate of an estimator. Consider the curved exponential family example where the parameter of interest is the solution manifold*

$$\Theta = \{\theta : \eta(\theta) - \eta_0 = 0\} \subset \mathbb{R}^d$$

such that

$$\eta_0 = \operatorname{argmax}_{\eta} \mathbb{E}(\log p(X; \eta))$$

is the population MLE. After observing IID random variables X_1, \dots, X_n , we obtain the sample MLE from the data

$$\widehat{\eta}_0 = \operatorname{argmax}_{\eta} \frac{1}{n} \sum_{i=1}^n \log p(X_i; \eta),$$

which leads to a manifold estimator

$$\widehat{\Theta}_n = \{\theta : \eta(\theta) - \widehat{\eta}_0 = 0\} \subset \mathbb{R}^d.$$

The stability theorem (Theorem 4) bounds the distance between $\widehat{\Theta}_n$ and Θ via the difference $\|\widehat{\eta}_0 - \eta_0\|$.

3. Monte Carlo approximation to solution manifolds. Given Ψ or its estimator/approximation $\widehat{\Psi}$, numerically finding the solution manifold M is a non-trivial task. In this section, we propose a simple gradient descent procedure to find a point on M . Note that though we describe the algorithm using Ψ , we will apply the algorithm to $\widehat{\Psi}$ in practice. Since M is the solution set of Ψ , we may rewrite it as

$$(3) \quad \begin{aligned} M &= \{x : \Psi(x) = 0\} = \{x : f(x) = 0\}, \\ f(x) &= \Psi(x)^T \Lambda \Psi(x), \end{aligned}$$

where Λ is an $s \times s$ positive definite matrix. Let x be an initial point. Consider the gradient flow $\pi_x(t)$:

$$\pi_x(0) = x, \quad \pi_x'(t) = -\nabla f(\pi_x(t)).$$

It is easy to see that points in M are stationary points of the gradient system; moreover, they are the minima of the function $f(x)$. Thus, we can use a gradient descent approach to find points on M . Algorithm 1 summarizes the gradient descent procedure for approximating M . Note that we may choose $\Lambda = \mathbb{I}$ to be the identity matrix. In this case, $f(x) = \|\Psi(x)\|^2$ so we will be investigating the gradient descent flow of $\|\Psi(x)\|^2$.

Algorithm 1 consists of three steps: a random initialization step, a gradient descent step, and a rejection step. The random initialization step allows us to explore different parts of the manifold.

Algorithm 1 Monte Carlo gradient descent algorithm

1. Randomly choose an initial point $x_0 \sim Q$, where Q is a distribution over the region of interest \mathbb{K} .
2. Iterates

$$(4) \quad x_{t+1} \leftarrow x_t - \gamma \nabla f(x_t)$$

until convergence. Let x_∞ be the convergent point.

3. If $\Psi(x_\infty) = 0$ (or sufficiently small), we keep x_∞ ; otherwise, discard x_∞ .
 4. Repeat the above procedure until we obtain enough points for approximating M .
-

The gradient descent step moves the initial points to possible candidates on M by iterating the gradient descent. The rejection step ensures that points being kept are indeed on the solution manifold.

Figure 1 shows an example of finding the solution manifold

$$\{(\mu, \sigma) : P(-5 < Y < 2) = 0.5, Y \sim N(\mu, \sigma^2)\}$$

using random initializations (from a uniform distribution over $[1, 3] \times [2, 4]$) and the gradient descent (later in Example 6, we will provide more details on the implementations). By using Algorithm 1, we can recover the underlying 1-dimensional manifold structure.

3.1. Analysis of the gradient flow. When an initial point is given, we perform gradient descent to find a minimum. To analyze this process, we start with an analysis of the (continuous-time) gradient flow $\pi_x(t)$. The gradient descent algorithm can be viewed as a discrete-time approximation to the continuous-time gradient flow. We introduce the following assumption to stabilize the gradient flow:

(F3) Λ is positive definite and $\Lambda_{\max}, \Lambda_{\min}$ are the largest and smallest eigenvalue of Λ .

(F3) is very mild since in most cases (such as the trivial case Λ is the identity matrix), Λ will be positive definite. With the additional assumption (F3), the function $f(x)$ has the following useful properties.

Lemma 5 *Assume (F1-3). Let $G_f(x) = \nabla f(x)$ and $H_f(x) = \nabla \nabla f(x)$ and $G_\psi(x) = \nabla \Psi(x) \in \mathbb{R}^{s \times d}$. Then we have the following properties:*

1. For each $x \in M$,
 - (a) the non-zero eigenvectors of $H_f(x)$ span the normal space of M at x .
 - (b) the minimal non-zero eigenvalue

$$\lambda_{\min, > 0}(H_f(x)) \geq \psi_{\min}^2(x) = \lambda_{\min, > 0}^2(G_\psi(x)^T G_\psi(x)) \Lambda_{\min} \geq 2\lambda_0^2 \Lambda_{\min}.$$

- (c) the minimal eigenvalue in the normal space of M at x $\lambda_{\min, \perp}(H_f(x)) = \lambda_{\min, > 0}(H_f(x))$.

2. Suppose that x has a unique projection $x_M \in M$ and let $N_M(x)$ be the normal space of M at x_M . If $d(x, M) < \delta_c = \min \left\{ \delta_0, \frac{\Lambda_{\min}}{8d\Lambda_{\max}} \frac{\lambda_0^2}{\|\Psi\|_{\infty, 2}^* \|\Psi\|_{\infty, 3}^*} \right\}$, then

$$\lambda_{\min, \perp, M}(H_f(x)) \equiv \min_{v \in N_M(x_M)} \frac{v^T H_f(x) v}{\|v\|^2} = \min_{v \in N_M(x_M)} \frac{\|H_f(x)v\|}{\|v\|} \geq \lambda_0^2 \Lambda_{\min}.$$

Property 1 in Lemma 5 describes the behavior of the Hessian $H_f(x)$ on the manifold. The eigenspace (corresponds to non-zero eigenvalues) is the same as the normal space of the manifold. With this insight, it is easy to understand property 1-(c) that the minimal eigenvalue in the normal space is the same as the minimal non-zero eigenvalue. Property 2 is about the behavior of $H_f(x)$ around the manifold. As long as we are sufficiently close to M , the Hessian $H_f(x)$ is well-behaved. The following theorem characterizes several important properties of the gradient flow.

Theorem 6 (Convergence of gradient flows) *Assume (F1-3). Let $\eta_x(t) = f(\pi_x(t))$ be the objective function along the flow and δ_c be defined in Lemma 5. Then the gradient flow $\pi_x(t)$ satisfies the following properties:*

1. (Convergence radius) For all $x \in M \oplus \delta_c$, $\pi_x(\infty) \in M$.
2. (Terminal flow orientation) Let $v_x(t) = \frac{\pi'_x(t)}{\|\pi'_x(t)\|}$ be the orientation of the gradient flow. If $\pi_x(\infty) \in M$, then $v_x(\infty) = \lim_{t \rightarrow \infty} v_x(t) \perp M$ at $\pi_x(\infty)$.
3. (Projection) For a sequence of points $\{x_n\}$ such that the initial level $\eta_{x_n}(0) = f(\pi_{x_n}(0)) = f(x_n) \rightarrow 0$,

$$\|x_n - \pi_{x_n}(\infty)\| = O(\sqrt{\eta_{x_n}(0)}).$$

The first result of Theorem 6 defines the convergence radius of the gradient flow. As long as the gradient flow is within δ_c distance to the manifold, the flow converges to the manifold. The second statement of the theorem characterizes the orientation of the gradient flow—the flow intersects the manifold from the normal space of the manifold. Namely, the flow hits the manifold orthogonally. The third statement shows that if the initial point has a low objective function value, then it must be close to the manifold at the order of the square root of the objective function value. If we choose $\Lambda = \mathbb{I}$ to be the identity matrix (F3 holds in this case), Theorem 6 implies the convergence of the gradient flow of $\|\Psi\|^2$.

Suppose that the initial point x is drawn from the distribution Q (that has a PDF q), the convergent point $\pi_x(\infty)$ can be viewed as a random draw from a distribution Q_M defined over the manifold M . The distribution Q and the distribution Q_M are associated via the mapping induced by the gradient descent process, so Q_M is a pushforward measure of Q (Bogachev, 2007). We now investigate how Q and Q_M are associated.

For every point $z \in M$, we define its basin of attraction (Chacón, 2015; Chen et al., 2016)

$$A(z) = \{x : \pi_x(\infty) = z\}.$$

Namely, $A(z)$ is the collection of initial points that the gradient flow converges to $z \in M$. Let $\mathcal{A}_M = \cup_{z \in M} A(z)$ be the union of all basins of attraction. The set \mathcal{A}_M characterizes the regions where the initialization leads to an accepted point in Algorithm 1. Thus, the acceptance probability of the rejection step of Algorithm 1 is $Q(\mathcal{A}_M) = \int_{\mathcal{A}_M} Q(dx)$.

The basin $A(z)$ has an interesting geometric property—it forms an s -dimensional manifold under smoothness assumption. This result is similar to the stable manifold theorem in dynamical systems literature (McGehee, 1973; McGehee and Sander, 1996; Banyaga and Hurtubise, 2013); in fact, it is more relevant to the local center manifold theorem (see, e.g., Section 2.12 of Perko 2001).

Theorem 7 (Local center manifold theorem) *Assume (F1-3). The basin of attraction $A(z)$ forms an s -dimensional manifold at each $z \in M$.*

An outcome from Theorem 7 is that the pushforward measure Q_M has an s -dimensional Hausdorff density function (Mattila, 1999; Preiss, 1987) if Q has a regular PDF q . Note that an s -dimensional

Hausdorff density at point x is defined through

$$\lim_{r \rightarrow 0} \frac{Q_M(B(x, r))}{C_s r^s},$$

where C_s is the s -dimensional volume of a unit ball. If the limit of the above equation exists, then Q_M has an s -dimensional Hausdorff density at point x .

Thus, if we obtain $Z_1, \dots, Z_N \in M$ from applying Algorithm 1, we may view them as IID observations from a distribution Q_M defined over the manifold M and this distribution Q_M has an s -dimensional Hausdorff density function. The model that we observed IID Z_1, \dots, Z_N from a distribution defined over a lower-dimensional manifold is common in computational geometry (Cheng et al., 2005b; Dey, 2006; Dey and Goswami, 2006; Chazal and Lieutier, 2008) so Theorem 7 implies that Algorithm 1 provides a new statistical example for this model.

3.2. Analysis of the gradient descent algorithm. In Algorithm 1, we do not perform the gradient descent using the flow π_x but instead, we use an iterative gradient descent approach that creates a sequence of discrete points $x_0, x_1, \dots, x_\infty$ such that

$$(5) \quad x_{t+1} = x_t - \gamma \nabla f(x_t), \quad x_0 = x,$$

where $\gamma > 0$ is the step size. Equation (5) defines the gradient descent algorithm.

It is well-known that if the step size γ is chosen incorrectly, the gradient descent algorithm will diverge. Thus, it is crucial to investigate what range of γ leads to a convergent point x_∞ and how fast the sequence $\{x_t : t = 0, 1, \dots\}$ converges to a point over M . The following theorem characterizes the algorithmic convergence along with a feasible range of the step size γ .

Theorem 8 (Linear convergence) *Assume (F1-3). When the initial point x_0 and step size γ satisfy*

$$d(x_0, M) < \delta_c = \min \left\{ \delta_0, \frac{\Lambda_{\min} \lambda_0^2}{8d \Lambda_{\max} \|\Psi\|_{\infty,2}^* \|\Psi\|_{\infty,3}^*} \right\},$$

$$\gamma < \min \left\{ \frac{1}{\Lambda_{\max} \|\Psi\|_{\infty,2}^*}, \frac{\Lambda_{\max} \|\Psi\|_{\infty,2}^*}{4\lambda_0^4 \Lambda_{\min}^2}, \delta_c \right\},$$

we have the following properties for $t = 0, 1, 2, \dots$:

$$f(x_t) \leq f(x_0) \cdot \left(1 - \gamma \frac{\lambda_0^4 \Lambda_{\min}^2}{\Lambda_{\max} \|\Psi\|_{\infty,2}^*} \right)^t,$$

$$d(x_t, M) \leq d(x_0, M) \left(1 - \gamma \lambda_0^2 \Lambda_{\min} \right)^{\frac{t}{2}}.$$

The convergence radius δ_c is the same as Theorem 6. Theorem 8 shows that when the initial point is within the convergence radius of the gradient flow and the step size is sufficiently small, the gradient descent algorithm converges linearly to a point on the manifold. An equivalent statement of Theorem 8 is that the algorithm takes only $O(\log(1/\epsilon))$ iterations to converge to ϵ -error to the minimum.

The key element in the derivation of Theorem 8 is to investigate the minimal eigenvalue of the normal space $\lambda_{\min, \perp}(H_f(x))$ for each $x \in M$. This quantity (appears in the theorem through

the lower bound $\lambda_0^2 \Lambda_{\min}$) controls the flattest direction of $f(x)$ in the normal space. The three requirements on the step sizes are for different reasons. The first requirement ($\gamma < \frac{1}{\Lambda_{\max} \|\Psi\|_{\infty,2}^*}$) is to make sure the objective function is decreasing. The second requirement ($\gamma < \frac{\Lambda_{\max} \|\Psi\|_{\infty,2}^*}{\lambda_0^2 \Lambda_{\min}}$) establishes the convergence rate. The third requirement ($\gamma < \delta_0$) ensures that the Hessian matrix behaves of f is well-behaved when applying the gradient descent algorithm. The first and the third requirement together is enough for showing that the gradient descent algorithm converges (but will not provide the convergence rate). To obtain the convergence rate, we need the additional second requirement.

Theorem 8 is a very interesting result—the function $f(x)$ is non-convex and but the gradient descent algorithm still converges linearly to a stationary point. An intuitive explanation of this result is that the function $f(x)$ is ‘directionally’ a convex function in the normal subspace of M (Property 2 in Lemma 5). Note that similar to Theorem 6, Theorem 8 applies to the gradient descent algorithm with $\Lambda = \mathbb{I}$ and in this case, (F3) is trivially true.

4. Statistical Applications.

4.1. *Likelihood inference.* One scenario that the solution manifolds will be useful is in likelihood inference. We provide three different examples showing how solution manifolds can be used in likelihood inference. Suppose that we observed IID observations X_1, \dots, X_n from some distribution P and we model the distribution using a parametric model P_θ and $\theta \in \Theta$. Let p_θ be the PDF/PMF of P_θ and let

$$\ell(\theta|X_1, \dots, X_n) = \frac{1}{n} \sum_{i=1}^n \log p_\theta(X_i)$$

be the log-likelihood function.

4.1.1. *Constrained MLE.* In likelihood inference, we may need to compute the MLE under some constraints. One example is the likelihood ratio test when the parametric space Θ_0 under H_0 is generated by equality constraints. Namely,

$$\Theta_0 = \{\theta \in \Theta : \Psi(\theta) = 0\}.$$

This problem occurs in algebraic statistic; see, e.g., Michałek et al. (2016) and Section 5 of Drton and Sullivan (2007).

To use the likelihood ratio test, we need to find the MLEs under both Θ_0 and Θ . Finding the MLE under Θ is a regular statistical problem. However, finding the MLE under Θ_0 may not be easy because of the constraint $\Psi(\theta) = 0$. Here we propose to use a procedure using gradient ascent of the likelihood function and gradient descent to the manifold to compute the constrained MLE. The procedure is described in Algorithm 2 and Figure 4 provides a graphical illustration. This algorithm consists of a one-step gradient ascent of the likelihood function (Step 3) and a gradient descent to manifold (Algorithm 1; Step 4 and 5).

The stopping criterion (Step 6) is that $\nabla \ell(\theta_\infty^{(m)}|X_1, \dots, X_n)$ belongs to the row space of $\nabla \Psi(\theta_\infty^{(m)})$. Due to Lemma 1, the row space of $\nabla \Psi(\theta_\infty^{(m)})$ is the normal space of M at $\theta_\infty^{(m)}$. It is easy to see that any critical points of the log-likelihood function on the manifold satisfy the condition that the likelihood gradient belongs to the row space of $\nabla \Psi$, so the constrained MLE is a stationary point in Algorithm 2. Hence we stop the algorithm when the stopping criterion occurs. However, other local modes and saddle points and local minima are also the stationary points so in practice, we

Algorithm 2 Manifold-constraint maximizing algorithm

1. Randomly choose an initial point $\theta_0^{(0)} = \theta_\infty^{(0)} \in \Theta$.
2. For $m = 1, 2, \dots$, do step 3-6:
3. **Ascent of likelihood.** Update

$$(6) \quad \theta_0^{(m)} = \theta_\infty^{(m-1)} + \alpha \nabla \ell(\theta_\infty^{(m-1)} | X_1, \dots, X_n),$$

where $\alpha > 0$ is the step size of the gradient ascent over likelihood function and $\ell(\theta | X_1, \dots, X_n)$ is the log-likelihood function.

4. **Descent to manifold.** For each $t = 0, 1, 2, \dots$ iterates

$$\theta_{t+1}^{(m)} \leftarrow \theta_t^{(m)} - \gamma \nabla f(\theta_t^{(m)})$$

until convergence. Let $\theta_\infty^{(m)}$ be the convergent point.

5. If $\Psi(\theta_\infty^{(m)}) = 0$ (or sufficiently small), we keep $\theta_\infty^{(m)}$; otherwise, discard $\theta_\infty^{(m)}$ and return to step 1.
 6. If $\nabla \ell(\theta_\infty^{(m)} | X_1, \dots, X_n)$ belongs to the row space of $\nabla \Psi(\theta_\infty^{(m)})$, we stop and output $\theta_\infty^{(m)}$.
-

need to run the algorithm with multiple initial points to increase the chance of finding the true MLE.

Note that one may replace the gradient ascent process by the EM algorithm. However, since the EM algorithm is not identical to a gradient ascent, it is unclear if the movement $\theta_0^{(m+1)} - \theta_\infty^{(m)}$ will be normal to the manifold Θ_0 or not.

Example 6 (Testing a tail probability in a Gaussian model) *To illustrate the idea, suppose that $X_i \in \mathbb{R}$ and the parametric distribution is a Gaussian $N(\mu, \sigma^2)$ with unknown mean and variance. Consider the null hypothesis*

$$H_0 : P(r_0 \leq Y \leq r_1) = s_0$$

for some given $s_0 > 0$ and r_0, r_1 (note that this example appears in Figure 1 as well). Let $\Phi(y) = P(Z \leq y)$ denotes the CDF of a standard normal. It is easy to see that H_0 forms the following constraint on (μ, σ^2) :

$$s_0 = \Phi\left(\frac{r_1 - \mu}{\sigma}\right) - \Phi\left(\frac{r_0 - \mu}{\sigma}\right).$$

Thus,

$$\Psi(\mu, \sigma) = \Phi\left(\frac{r_1 - \mu}{\sigma}\right) - \Phi\left(\frac{r_0 - \mu}{\sigma}\right) - s_0 \in \mathbb{R}$$

so the feasible set of (μ, σ^2) forms a 1D solution manifold in \mathbb{R}^2 . It is difficult to find the analytical form of the MLE under H_0 but we may use the method in Algorithm 2 to obtain a numerical approximation to it. In particular, the derivative of $\Psi(\mu, \sigma)$ with respect to μ and σ has the following closed-form:

$$\begin{aligned} \frac{\partial}{\partial \mu} \Psi(\mu, \sigma) &= -\frac{1}{\sigma} \phi\left(\frac{r_1 - \mu}{\sigma}\right) + \frac{1}{\sigma} \phi\left(\frac{r_0 - \mu}{\sigma}\right) \\ \frac{\partial}{\partial \sigma} \Psi(\mu, \sigma) &= -\frac{r_1 - \mu}{\sigma^2} \phi\left(\frac{r_1 - \mu}{\sigma}\right) + \frac{r_0 - \mu}{\sigma^2} \phi\left(\frac{r_0 - \mu}{\sigma}\right), \end{aligned}$$

where $\phi(y) = \frac{1}{\sqrt{2\pi}} e^{-y^2/2}$ is the PDF of the standard normal. With the above derivatives, it is easy to implement Algorithm 2. Figure 4 shows an example of applying Algorithm 2. to this example with $r_1 = -5, r_2 = 2$ and $s_0 = 0.5$ (and 1000 random numbers generated from $N(1.5, 3^2)$). All the five random initial points converge to the maximum on the manifold.

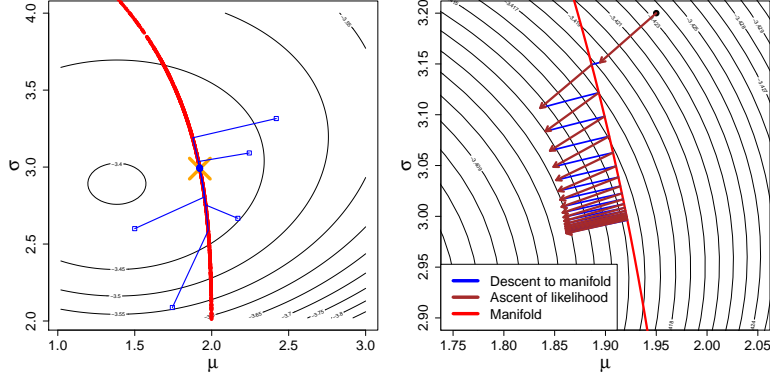


FIG 4. An example illustrating how Algorithm 2 works. We consider the example of estimating the tail probability in a Gaussian model $N(\mu, \sigma^2)$ with the constraint $P(-5 \leq X \leq 2) = 0.5$. We generate $n = 1000$ points from $N(1.5, 3^2)$ and display the log-likelihood function in the two panels (contours are the log-likelihood surface). **Left:** We initialize Algorithm 2 with 5 random points (blue boxes) and the algorithm creates an ascending path (blue lines) to the maximum point (orange cross). **Right:** We illustrate the Algorithm 2 by showing points in each iteration in the algorithm in a zoom-in area relative to the left panel. Starting from the solid black point, we first perform a gradient ascent with respect to the log-likelihood function (brown arrow) then we apply Algorithm 1 to descent to the solution manifold. We keep repeating this process until it converges.

4.1.2. *Mixture models with moment constraints.* The mixture models with moment constraints (Lindsay, 1995; Chauveau and Hunter, 2013) is another scenario where solution manifolds occur in a parametric model. Suppose that we are modeling the observations $X_1, \dots, X_n \in \mathbb{R}$ as IID from a mixture model

$$\sum_{\ell=1}^L \omega_{\ell} p(x; \theta_{\ell}),$$

where $\omega_{\ell} \geq 0$ and $\sum_{\ell=1}^L \omega_{\ell} = 1$ are the weight for ℓ -th component and $\theta_{\ell} \in \Theta_{\ell}$ is the parameter of the ℓ -th component. The total parameter space is

$$\Theta = \left\{ (\omega_1, \dots, \omega_L, \theta_1, \dots, \theta_L) : \omega_{\ell} \geq 0, \sum_{\ell=1}^L \omega_{\ell} = 1, \theta_j \in \Theta_j, j = 1, \dots, L \right\}.$$

Note that Θ has a total of $\|\Theta\| = (L-1) + \sum_{\ell=1}^L \|\Theta_{\ell}\|$ numbers of free parameters. A conventional approach of parameter estimation is via the MLE of the mixture model.

However, the MLE is not the only approach for estimating the parameter. The method of moments is another popular approach for parameter estimation. In the mixture model, the k -th moment can be succinctly expressed as

$$(7) \quad \mathbb{E}(X^k) = \sum_{\ell=1}^L \omega_{\ell} \cdot \mu_{k,\ell}(\theta_{\ell}), \quad \mu_{k,\ell} = \int x^k p(x; \theta_{\ell}) dx$$

and often $\mu_{k,\ell}$ has a simple closed form. By matching moments up to $\|\Theta\|$ -th moments, we obtain a moment estimator.

If we do not match all moments up to the $\|\Theta\|$ -th moment, the moment equations from equation (7) lead to a solution manifold in the parameter space. This implies that we may combine both the

method of moments and the MLE to obtain an ML estimator that matches the moment constraints. Specifically, consider the estimator

$$\begin{aligned} \hat{\theta}_{\text{MLE},k} &= \operatorname{argmax}_{\theta \in \Theta} \sum_{i=1}^n \log \left(\sum_{\ell=1}^L \omega_{\ell} \cdot p(x; \theta_{\ell}) \right) \\ \text{subject to} \quad & \frac{1}{n} \sum_{i=1}^n X_i^j = \sum_{\ell=1}^L \omega_{\ell} \cdot \mu_{j,\ell}(\theta_{\ell}), j = 1, \dots, k. \end{aligned}$$

The model from $\hat{\theta}_{\text{MLE},k}$ matches all the k -th empirical moments to the data and has the highest likelihood value compared to all models satisfying the moment constraints. Numerically, we can use Algorithm 2 to compute this moment-matching MLE.

4.1.3. *Curved exponential family.* Curved exponential family (Efron, 1975, 1978) is a collection of parametric models such that the density has the form of

$$p_{\theta}(x) = \frac{1}{Z(\theta)} \exp(T(x)^T \eta(\theta)), \quad Z(\theta) = \int \exp(T(x)^T \eta(\theta)) dx,$$

where the parameter of model $\eta \in \Xi \subset \mathbb{R}^s$, and $\theta \in \Theta \subset \mathbb{R}^d$ and $T(x) = (T_1(x), \dots, T_s(x))$ are the sufficient statistics. Most of the work on curved exponential families focus on the case $d < s$ so that the model $\{\eta = \eta(\theta) : \theta \in \Theta\}$ forms a d -dimensional manifold within \mathbb{R}^s .

However, in reality, there may be more parameters than the model parameter that generates our data. Namely, $s < d$. In this situation, the data only provides constraints one the parameter space but does not uniquely determine a single estimate. Let

$$\hat{\eta}_{\text{MLE}} = \operatorname{argmax}_{\eta \in \Xi} \ell(\eta | X_1, \dots, X_n)$$

be the MLE of the model parameter. This MLE implies a solution manifold under Θ as

$$\hat{\Theta}_{\text{MLE}} = \{\theta \in \Theta : 0 = \eta(\theta) - \hat{\eta}_{\text{MLE}}\},$$

which is a $(d - s)$ -dimensional solution manifold with $\hat{\Psi}(\theta) = \eta(\theta) - \hat{\eta}_{\text{MLE}}$. Thus, the framework we developed can be readily applied to this problem. Algorithm 1 offers a simple way to generate feasible points on $\hat{\Theta}_{\text{MLE}}$. Econometrics

The stability theory in Theorem 4 implies that $\hat{\Theta}_{\text{MLE}}$ converges to a population MLE $\Theta_{\text{MLE}} = \{\theta \in \Theta : 0 = \eta(\theta) - \eta_{\text{MLE}}\}$, where $\eta_{\text{MLE}} = \operatorname{argmax}_{\eta \in \Xi} \mathbb{E}(\ell(\eta | X_1))$, under the Hausdorff distance.

4.2. *Partial identification and generalized method of moments.* The solution manifolds appear in the partial identification problem (Manski, 2003) in Econometrics. One example is the moment constraint problem (Chernozhukov et al., 2007), also known as the generalized method of moments (Hansen, 1982; Hansen and Singleton, 1982), where we want to estimate parameter $\theta \in \mathbb{R}^d$ that solves the moment equation

$$\mathbb{E}(g(Y; \theta)) = 0,$$

where $g(y; \theta) \in \mathbb{R}^s$ is a vector-valued function and X is a random variable denoting the observed data. It is easy to see that when $s < d$, the solution set (also called an identified set in Chernozhukov et al. 2007) $M = \{\theta : \mathbb{E}(f(Y; \theta)) = 0\}$ forms a solution manifold.

Thus, the smoothness theorem (Theorem 3) and the stability theorem (Theorem 4) can be applied to this case. In particular, when the estimator is obtained by the empirical moment equation, i.e.,

$$\widehat{M}_n = \left\{ \theta : \frac{1}{n} \sum_{i=1}^n f(Y_i; \theta) = 0 \right\}.$$

Theorem 4 implies that

$$\text{Haus}(\widehat{M}_n, M) \xrightarrow{P} 0$$

when the empirical moments $\frac{1}{n} \sum_{i=1}^n f(Y_i; \theta)$ and its derivatives with respect to θ converges to the population moments $\mathbb{E}(g(X; \theta))$ and its derivatives, respectively.

In generalized method of moments, a common approach of finding a solution to $\mathbb{E}(g(Y; \theta)) = 0$ is via minimizing a criterion function $Q(\theta) = \mathbb{E}(g(Y; \theta))^T \Lambda \mathbb{E}(g(Y; \theta))$, where Λ is a positive definite matrix (Hansen and Singleton, 1982). This is identical to the function f defined in equation (3). Thus, the analysis in Section 3 can be used to study the minimization problem in the generalized method of moments.

Remark 2 *In econometrics, a similar problem to the solution manifold is the inequality constraint problem, which occurs when we replace the equality constraints with inequality constraints (Tamer, 2010; Romano and Shaikh, 2010), i.e.,*

$$\mathbb{E}(g_\ell(Y; \theta)) \leq 0$$

for $\ell = 1, \dots, s$. The goal is to find θ satisfying the above inequality constraint. A common approach to finding the feasible set is via defining an objective function

$$Q(\theta) = \left| \sum_{\ell=1}^s [\mathbb{E}(g_\ell(Y; \theta))]_+ \right|^2, \quad [y]_+ = \max(y, 0)$$

so that the feasible set is $\{\theta : Q(\theta) = 0\}$. The inequality constraint implies that $\{\theta : Q(\theta) = 0\}$ may not form a lower-dimensional manifold but a subset of the original parameter space.

A common estimator of $\{\theta : Q(\theta) = 0\}$ is

$$\left\{ \theta : \widehat{Q}_n(\theta) \leq c_n \right\}, \quad \widehat{Q}_n(\theta) = \left| \sum_{\ell=1}^s \left[\frac{1}{n} \sum_{i=1}^n g_\ell(Y_i; \theta) \right]_+ \right|^2$$

for some sequence $c_n \rightarrow 0$. Note that by properly choosing c_n , we may construct both an estimator and a confidence region; see Chernozhukov et al. (2007) and Romano and Shaikh (2010) for more details.

4.3. Bayesian inference. The techniques we develop for solution manifolds can be used for Bayesian inference after some modifications. One example is the univariate Gaussian with unknown mean μ and variance σ^2 and we have a second moment constraint so the parameter space is $\Theta(s_0) = \{(\mu, \sigma^2) : \mathbb{E}(Y^2) = \mu^2 + \sigma^2 = s_0^2\}$. We can place a prior $\pi(\theta)$ over $\Theta(s_0)$ that reflects our prior belief about the parameter $\theta = (\mu, \sigma)$. However, how to sample from π (and the posterior) is a non-trivial task because π is supported on a manifold.

The Monte Carlo approximation method in Section 3 offers a solution to sampling from π . With a little modification of Algorithm 1, we can approximate the posterior distribution defined on the

Algorithm 3 Approximated manifold posterior algorithm

1. Apply Algorithm 1 to generate many points $Z_1, \dots, Z_N \in M$.
2. Estimate a density score of Z_i using

$$\hat{\rho}_{i,N} = \frac{1}{N} \sum_{j=1}^N K\left(\frac{\|Z_i - Z_j\|}{h}\right),$$

where $h > 0$ is a tuning parameter and K is a smooth function such as a Gaussian.

3. Compute the posterior density score of Z_i as

$$(8) \quad \hat{\omega}_{i,N} = \frac{1}{\hat{\rho}_{i,N}} \cdot \hat{\pi}_{i,N}, \quad \hat{\pi}_{i,N} = \pi(Z_i) \cdot \prod_{j=1}^n p(X_j|Z_i),$$

return Weighted point clouds $(Z_1, \hat{\omega}_{1,N}), \dots, (Z_N, \hat{\omega}_{N,N})$.

solution manifold. Let π be a prior PDF defined over the solution set $M = \{\theta : \Psi(\theta) = 0\}$ where $\Psi : \Theta \mapsto \mathbb{R}^k$ and we observe IID observations X_1, \dots, X_n that are assumed to be from a parametric model $p(x|\theta)$. The posterior distribution of θ will be

$$\pi(\theta|X_1, \dots, X_n) \propto \begin{cases} \pi(\theta) \prod_{i=1}^n p(X_i|\theta), & \text{if } \theta \in M; \\ 0, & \text{if } \theta \notin M. \end{cases}$$

Here we propose a method that approximates the posterior distribution using a weighted point cloud. Our approach is formally described in Algorithm 3. Note that the algorithm we develop only requires the ability to evaluate a function $\rho(\theta) \propto \pi(\theta)$; we do not need the exact value of the prior density.

Example 7 (Bayesian analysis of Example 6) *Figure 5 shows an example of 90% credible intervals and the MAPs under three scenarios: prior distribution only (left panel), posterior distribution with $n = 100$ (middle panel) and posterior distribution with $n = 1000$ (right panel). This is the same setting in Example 6 and Figure 4 that the manifold is formed by the constraint $P(-5 < X < 2) = 0.5$ with $X \sim N(\mu, \sigma)$. We choose the prior distribution (density) as*

$$\pi(\mu, \sigma) \propto \phi(\mu; 2, 0.2)\phi(\sigma; 2.5, 0.2)I((\mu, \sigma) \in M),$$

where $\phi(x; a, b)$ is the density of $N(a, b^2)$. In the left panel, the credible interval is completely determined by the prior distribution and the MAP is the mode of the prior. In the middle and the right panels, the data is incorporated into the posterior distributions; both the credible intervals and MAPs are changing due to the influence of the data. Our method (Algorithm 3 and equation (10)) provides a simple and elegant way of approximating the credible intervals on the manifold.

To see why the outputs from Algorithm 3 are a valid approximation to the posterior density, note that the density score $\hat{\rho}_{i,N}$ is proportional to the underlying density of Z_1, \dots, Z_M defined over M . So the weighted point cloud $(Z_1, \hat{\rho}_{1,N}^{-1}), \dots, (Z_N, \hat{\rho}_{N,N}^{-1})$ behaves like a uniform sample over M . Thus, to account for the unweighted point cloud density, we have to rescale the posterior score of Z_i in equation (8) by the factor $\hat{\rho}_{i,N}^{-1}$. Note that the value $\hat{\pi}_{i,N}$ is proportional to the posterior density $\pi(Z_i|X_1, \dots, X_n)$ evaluated at point $\theta = Z_i$.

With the output from Algorithm 3, the posterior density $\pi(\theta|X_1, \dots, X_n)$ are represented by the collection of points Z_1, \dots, Z_N along with the corresponding weights $\hat{\omega}_{1,N}, \dots, \hat{\omega}_{N,N}$. The posterior mean can be approximated using

$$\hat{\theta}_{\text{Pmean}} = \frac{\sum_{i=1}^n \hat{\omega}_{i,N} Z_i}{\sum_{i=1}^n \hat{\omega}_{i,N}}.$$

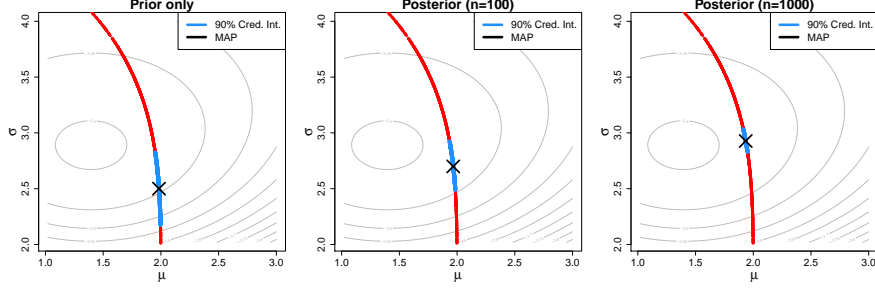


FIG 5. An example showing the credible interval (credible region) and MAP on the manifold. We use the same example in Figure 4 and the prior distribution $\pi(\mu, \sigma) \propto \phi(\mu; 2, 0.2)\phi(\sigma; 2.5, 0.2)I((\mu, \sigma) \in M)$, where $\phi(x; a, b)$ is the density of $N(a, b^2)$. **Left:** the 90% credible interval along with the MAP using only the prior distribution. **Middle:** we randomly generate $n = 100$ observations from $N(1.5, 3^2)$ and compute 90% credible interval and MAP from the posterior distribution. **Right:** the same analysis as the middle panel but now we use a sample of size $n = 1000$. Note that the background gray contours show the log-likelihood function (as an indication of how the likelihood function will influence posterior).

This estimator is essentially the importance sampling estimator. The posterior mode (MAP: maximum a posteriori) can be approximated using

$$\hat{\theta}_{\text{MAP}} = Z_{i^*}, \quad i^* = \operatorname{argmax}_{i \in \{1, \dots, N\}} \hat{\pi}_{i, N}.$$

The weighted point cloud also leads to an approximated credible region. Let $1 - \alpha$ be the credible level and $Z_{(1)}, \dots, Z_{(N)}$ be the ordered points such that

$$\hat{\pi}_{(1), N} \geq \hat{\pi}_{(2), N} \geq \dots \geq \hat{\pi}_{(N), N}.$$

Define

$$(9) \quad i(\alpha) = \operatorname{argmin} \left\{ i : \frac{\sum_{j=1}^i \hat{\omega}_{(j), N}}{\sum_{\ell=1}^N \hat{\omega}_{(\ell), N}} \geq 1 - \alpha \right\}.$$

Then we may use the collection of points

$$(10) \quad \{Z_{(1)}, \dots, Z_{(i(\alpha))}\}$$

as an approximation of a $1 - \alpha$ credible region. Alternatively, one may use the set

$$\{\theta \in M : \pi(\theta | X_1, \dots, X_n) \geq \pi(Z_{(i(\alpha))} | X_1, \dots, X_n)\}$$

as another approximation of a $1 - \alpha$ credible region.

Here is an explanation of the choice in equation (9). Since $\hat{\pi}_{i, N}$ is proportional to the posterior value at Z_i , we have

$$\pi(Z_{(1)} | X_1, \dots, X_n) \geq \pi(Z_{(2)} | X_1, \dots, X_n) \geq \dots \geq \pi(Z_{(N)} | X_1, \dots, X_n).$$

Define the upper-level set of level λ of the posterior distribution as

$$L(\lambda) = \{\theta : \pi(\theta | X_1, \dots, X_n) \geq \lambda\}.$$

It is easy to see that the posterior probability within $L(\lambda)$ is

$$\pi(L(\lambda)|X_1, \dots, X_n) = \int I(\theta \in L(\lambda))\pi(\theta|X_1, \dots, X_n)d\theta.$$

An $1 - \alpha$ credible region will be choosing the minimal value λ_α such that

$$(11) \quad \lambda_\alpha = \inf \{ \lambda : \pi(L(\lambda)|X_1, \dots, X_n) \geq 1 - \alpha \}.$$

With the weights $\hat{\omega}_{1,N}, \dots, \hat{\omega}_{N,N}$, an approximation to $\pi(L(\lambda)|X_1, \dots, X_n)$ is

$$\hat{\pi}(L(\lambda)|X_1, \dots, X_n) = \frac{\sum_{j=1}^n \hat{\omega}_{j,N} I(Z_j \in L(\lambda))}{\sum_{\ell=1}^n \hat{\omega}_{\ell,N}}.$$

The posterior levels $\hat{\pi}_{1,N}, \dots, \hat{\pi}_{N,N}$ form a discrete approximation of all levels of λ . Thus, an approximation to equation (11) is

$$\begin{aligned} \hat{\lambda}_\alpha &= \min \left\{ \hat{\pi}_{i,N} : \frac{\sum_{j=1}^n \hat{\omega}_{j,N} I(Z_j \in L(\hat{\pi}_{i,N}))}{\sum_{\ell=1}^n \hat{\omega}_{\ell,N}} \geq 1 - \alpha \right\} \\ &= \min \left\{ \hat{\pi}_{i,N} : \frac{\sum_{j=1}^n \hat{\omega}_{j,N} I(\hat{\pi}_{j,N} \geq \hat{\pi}_{i,N})}{\sum_{\ell=1}^n \hat{\omega}_{\ell,N}} \geq 1 - \alpha \right\} \\ &= \min \left\{ \hat{\pi}_{(i),N} : \frac{\sum_{j=1}^i \hat{\omega}_{(j),N}}{\sum_{\ell=1}^n \hat{\omega}_{(\ell),N}} \geq 1 - \alpha \right\} \\ &= \hat{\pi}_{(i(\alpha)),N}, \quad i(\alpha) = \operatorname{argmin} \left\{ i : \frac{\sum_{j=1}^i \hat{\omega}_{(j),N}}{\sum_{\ell=1}^n \hat{\omega}_{(\ell),N}} \geq 1 - \alpha \right\}. \end{aligned}$$

Thus, the choice in equation (9) is from the above approximation to the level λ_α .

Remark 3 Note that the posterior mean may not be on the manifold so one may replace it by the posterior Fréchet mean (Grove and Karcher, 1973), which is defined as

$$\hat{\theta}_{\text{PFmean}} = Z_{i^\dagger}, \quad i^\dagger = \operatorname{argmin}_{i \in \{1, \dots, N\}} \sum_{j=1}^N \hat{\omega}_{j,N} (Z_i - Z_j)^2.$$

The Fréchet mean defines a mean of a random variable X using the minimization problem $\operatorname{argmin}_\mu E(X - \mu)^2$ and constrains the minimizer to be in the manifold. Here we use the weighted point approximation to this minimization.

4.4. *Nonparametric set estimation.* Solution manifolds occur in many scenarios of nonparametric set estimation problems. One famous example is the density level set problem where the parameter of interest is the (density) level set $\{x : p(x) = \lambda\}$ and p is the PDF that generates our data and λ is a pre-specified level. In this case, the smoothness theorem (Theorem 3) yields the same result as Chen et al. (2017) and the stability theorem (Theorem 4) suggests that the convergence rate under the Hausdorff distance will be the rate of estimating the density function, which is consistent with several existing work (Cadre, 2006; Rinaldo and Wasserman, 2010; Rinaldo et al., 2012).

Interestingly, most of the past literature on level set problems do not consider the algorithmic aspect of finding a level set but this is a non-trivial task in the multivariate cases because the number

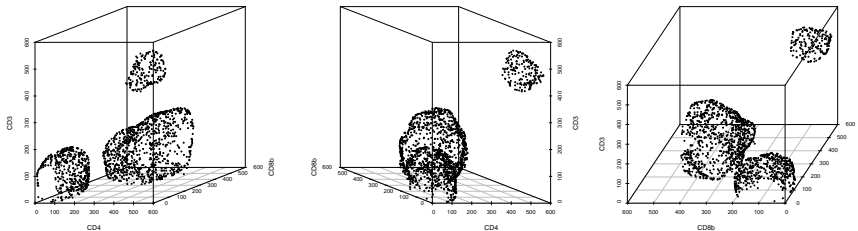


FIG 6. An example of approximating a density level set. This is the GvHD data that we borrowed from `mclust` package in R. We use the control group and choose three variables: CD3, CD4, CD8b. We apply a Gaussian kernel density estimator with bandwidth $h = 20$ (same in all coordinates). The level set of interest is the density level corresponds to 25% quantile of densities at all observations. The three panels display the level set under three different angles.

of grid cells increases exponentially with respect to the dimension. The methods we developed in Section 3 can be used to find points on the level set. As an illustration, Figure 6 shows an example of approximating the level set using Algorithm 1 with the Graft-versus-Host Disease (GvHD) data (Brinkman et al., 2007) from `mclust` package in R (Baudry et al., 2010). We use variables CD3, CD4, and CD8b and focus on the control group. The density is computed using a Gaussian kernel density estimator with equal bandwidth $h = 20$ in all coordinates. We choose the level as the 25% quantile of all observations' densities. The three panels display the approximated level sets from three angles. The three surfaces in the data indicate that there are three connected components in the regions where the density is above this threshold.

In addition to the level set problem, density ridges (Chen et al., 2015; Genovese et al., 2014) are also examples of solution manifolds. The density k -ridges are the collection $\{x : V_k(x)^T \nabla p(x) = 0, \lambda_k(x) < 0\}$, where $V_k(x) = [v_k(x), \dots, v_d(x)]$ are the matrix of $d - k$ eigenvectors of $\nabla \nabla p(x)$ corresponding to the lowest eigenvalues and $\lambda_k(x)$ is the k -th largest eigenvalue. It is easy to see that if we only pick the lowest $d - k$ eigenvectors, we obtain a system of equations with $d - k$ equations, leading to a k -dimensional manifold (under smoothness conditions). The stability theorem (Theorem 4) states that the convergence rate of a density ridge estimator will be at the rate of estimating the Hessian matrix, which is consistent with the findings in Genovese et al. (2014).

5. Discussion. In this paper, we study the properties of the solution manifold. We show that when the generating function $\Psi(x)$ is at least three-times continuously differentiable, the solution manifold is smooth and is stable under small perturbation. Also, we introduce a Monte Carlo gradient descent algorithm that allows us to approximate a solution manifold by a point cloud. We show that the algorithm converges linearly to a point on the manifold. We also demonstrate how solution manifolds are relevant to many statistical problems. We propose a method for finding MLE on the solution manifold and a procedure for approximating a posterior distribution defined over the manifold. In what follows, we discuss some relevant topics to the solution manifolds.

5.1. *Smoothness, stability, and convergence of gradient flow.* In this paper, we developed 5 major theoretical results: the smoothness theorem (Theorem 3), stability theorem (Theorem 4), gradient flow theorem (Theorem 6), local center manifold theorem (Theorem 7), and the algorithmic convergence theorem (Theorem 8). These results are characterizing different properties of the

solution manifolds are often studied in various fields, ranging from computational geometry, statistics, dynamical systems to optimization. In our work, we showed that they all rely on the same set of assumptions: (F1) the smoothness of Ψ and (F2) the curvature assumption of Ψ around M .

Assumption (F1) is more than enough for some theoretical results. The smoothness theorem can be relaxed to assuming that Ψ satisfies β -Hölder condition with $\beta \geq 2$. The stability theorem only requires Ψ being β -Hölder with $\beta > 2$. The requirement of the third derivative (can be replaced by β -Hölder with $\beta \geq 3$) is needed only in the case of analyzing a gradient flow. Thus, there is a hierarchy of smoothness that corresponds to different theoretical results. The smoothness of M requires the least condition, and then is the stability of M , and then is the convergence of gradient flow.

In statistics, we often assume conditions similar to (F1-2) to establish a stability theorem, which leads to the convergence rate of a plug-in estimate. The analysis from this paper shows that slightly relaxing the assumptions leads to a smoothness population quantity and a well-behaved gradient system, which implies that we can use the idea of gradient descent to approximate the estimator numerically. In fact, under a mild modification of the proofs, one can derive all these 5 theorems for a regular Z -estimator.

5.2. *Connections to other fields.* We would like to point out that the results of this paper have several connections to other fields.

- **Econometrics.** Solution manifolds occur in the partial identification problem (Section 4.2) so our analysis provides some insights into the moment equality constraint problem (Chernozhukov et al., 2007). Also, our analysis on the gradient descent (e.g., Theorem 6) can be applied to investigating the property of the minimization problem in the generalized method of moments approach (Hansen, 1982; Hansen and Singleton, 1982).
- **Dynamical systems.** As is mentioned before, Theorem 7 is related to the stable manifold theorem and the local center manifold theorem in dynamical systems (McGehee, 1973; McGehee and Sander, 1996; Banyaga and Hurtubise, 2013; Perko, 2001). Our analysis provides statistical examples that these theorems may be useful in data analysis.
- **Computational geometry.** If we stop the gradient descent process early, we do not obtain points that are on the manifold. The resulting points may be viewed as $Z_i = X_i + \epsilon_i$, where $X_i \in M$ is from a distribution over the manifold and ϵ_i is some additive noise. This model is a common additive noise model in computational geometry literature (Cheng et al., 2005b,a; Dey, 2006; Dey and Goswami, 2006; Chazal and Lieutier, 2008; Boissonnat and Ghosh, 2014). Our proposed method provides another concrete example of the manifold additive noise model.
- **Optimization.** In general, a gradient descent method has a linear convergence rate when the objective function is strongly convex and has a smooth gradient (Boyd and Vandenberghe, 2004; Nesterov, 2018). However, in our setting, the objective function $f(x)$ is non-convex (and is not locally convex) but the gradient descent algorithm still obtains a linear (algorithmic) convergence rate (Theorem 6). This reveals a class of non-convex objective functions that can still be minimized quickly using a gradient descent algorithm.

5.3. *Future work.* The framework we developed in this paper has many potentials in other problems. Here we provide some possible directions that we plan to pursue in the future.

- **Log-linear model.** The log-linear model of categorical variables is an interesting example in the sense that it can be expressed as a solution manifold when there are constraints like conditional independence but it may be unnecessary to use the techniques developed

in this paper. Consider a d -dimensional categorical random vector X that takes values in $\{0, 1, 2, \dots, J-1\}^d$. The joint PMF of X $p(x_1, \dots, x_d)$ has J^d entries with the constraint that $\sum_x p(x_1, \dots, x_d) = 1$ so it has $J^d - 1$ degrees of freedom. In the log-linear model, we reparametrize the PMF using the log-linear expansion: $\log p(x) = \sum_A \psi_A(x_A)$, where A is any non-empty subset of $\{1, 2, \dots, J\}$ and $x_A = (x_j : j \in A)$ with the constraint that $\psi_A(x_A) = 0$ if any $x_j = 0$ for $j \in A$. Under the log-linear model, we reparametrize the joint PMF using the parameters $\Theta_{\text{LL}} = \{\psi_A(x_A) : A \subset \{1, 2, \dots, J\}, x_A \in \{0, 1\}^{|A|}\}$, where $|A|$ is the cardinality of A . When there is constraint, the feasible parameters in Θ_{LL} forms a solution manifold. However, common constraints in the log-linear model are that interaction terms $\psi_A = 0$ for some A . This leads to a flat manifold so there is no need to use the technique developed in this paper. We may need to use techniques from the solution manifold when the constraint is placed on the PMF $p(x_1, \dots, x_d)$ rather than the log-linear models since constraints on the PMF leads to an implicit constraint on Θ_{LL} . We leave this as future work.

- **Confidence regions of solution manifolds.** Another future direction is to develop a method for constructing the confidence regions of solution manifolds. In the construction of a confidence region of a set, there are two common approaches. The first one is based on the ‘vertical uncertainty’—the uncertainty due to $\widehat{\Psi} - \Psi$. This idea has been applied in generalized method of moment problems (Chernozhukov et al., 2007; Romano and Shaikh, 2010) and level set estimations (Mammen and Polonik, 2013; Qiao and Polonik, 2019; Cheng et al., 2019). The other approach is based on the ‘horizontal uncertainty’—the uncertainty due to $\text{Haus}(\widehat{M}, M)$. This technique has been used in constructing confidence sets of density ridges and level sets (Chen et al., 2015, 2017). Based on these results, we believe that it is possible to develop a procedure for constructing confidence regions of solution manifolds and we leave this as future work.
- **A new class of non-convex problems.** In Theorem 8, we observe an interesting phenomenon—although the objective function $f(x) = \Psi^T \Lambda \Psi(x)$ is non-convex, we still obtain a linear (algorithmic) convergence. Note that for a non-convex function but locally convex around the minimizer, the linear convergence can be established via assuming a local strongly-convexity of the objective function (Balakrishnan et al., 2017), i.e., $f(x)$ is strongly-convex within $B(x^*, r)$ for some radius $r > 0$ and x^* is the global minimizer. However, our problem is more complicated in the sense that $f(x)$ is flat along M so it is not locally strongly convex. The key element in our result is the assumption (F2): $f(x)$ behaves like being ‘locally strongly-convex’ in the normal direction of M . Thus, with some additional structure on the non-convex function, we may still obtain a fast convergence rate. We will investigate how this may be useful in other non-convex optimization problems. Also, the analysis may be applied to other forms of $f(x)$ that are not limited to a ‘squared’-type transformation of $\Psi(x)$ ($f(x)$ behaves like the square of Ψ), which may further improve the convergence rate. For instance, the gradient descent over $f_1(x) = \|\Psi(x)\|_1$ may also converge faster than over the function $f(x)$. We will investigate this in the future.

Acknowledgements. We thank M. Drton for helpful comments. YC is partially supported by NSF grant DMS 1810960 and NIH grant U01 AG016976.

REFERENCES

- S. Balakrishnan, M. J. Wainwright, and B. Yu. Statistical guarantees for the em algorithm: From population to sample-based analysis. *The Annals of Statistics*, 45(1):77–120, 2017.
- A. Banyaga and D. Hurtubise. *Lectures on Morse homology*, volume 29. Springer Science & Business Media, 2013.

- J.-P. Baudry, A. E. Raftery, G. Celeux, K. Lo, and R. Gottardo. Combining mixture components for clustering. *Journal of computational and graphical statistics*, 19(2):332–353, 2010.
- V. I. Bogachev. *Measure theory*, volume 1. Springer Science & Business Media, 2007.
- J.-D. Boissonnat and A. Ghosh. Manifold reconstruction using tangential delaunay complexes. *Discrete & Computational Geometry*, 51(1):221–267, 2014.
- S. Boyd and L. Vandenberghe. *Convex optimization*. Cambridge university press, 2004.
- R. R. Brinkman, M. Gasparetto, S.-J. J. Lee, A. J. Ribickas, J. Perkins, W. Janssen, R. Smiley, and C. Smith. High-content flow cytometry and temporal data analysis for defining a cellular signature of graft-versus-host disease. *Biology of Blood and Marrow Transplantation*, 13(6):691–700, 2007.
- B. Cadre. Kernel estimation of density level sets. *Journal of multivariate analysis*, 97(4):999–1023, 2006.
- J. E. Chacón. A population background for nonparametric density-based clustering. *Statistical Science*, 30(4):518–532, 2015.
- D. Chauveau and D. Hunter. Ecm and mm algorithms for normal mixtures with constrained parameters. 2013.
- F. Chazal and A. Lieutier. The “ λ -medial axis”. *Graphical Models*, 67(4):304–331, 2005.
- F. Chazal and A. Lieutier. Smooth manifold reconstruction from noisy and non-uniform approximation with guarantees. *Computational Geometry*, 40(2):156–170, 2008.
- Y.-C. Chen, C. R. Genovese, and L. Wasserman. Asymptotic theory for density ridges. *The Annals of Statistics*, 43(5):1896–1928, 2015.
- Y.-C. Chen, C. R. Genovese, and L. Wasserman. A comprehensive approach to mode clustering. *Electronic Journal of Statistics*, 10(1):210–241, 2016.
- Y.-C. Chen, C. R. Genovese, and L. Wasserman. Density level sets: Asymptotics, inference, and visualization. *Journal of the American Statistical Association*, 112(520):1684–1696, 2017.
- G. Cheng, Y.-C. Chen, et al. Nonparametric inference via bootstrapping the debiased estimator. *Electronic Journal of Statistics*, 13(1):2194–2256, 2019.
- S.-W. Cheng, T. K. Dey, and E. A. Ramos. Manifold reconstruction from point samples. In *SODA*, volume 5, pages 1018–1027, 2005a.
- S.-W. Cheng, S. Funke, M. Golin, P. Kumar, S.-H. Poon, and E. Ramos. Curve reconstruction from noisy samples. In *Computational Geometry 31*, 2005b.
- V. Chernozhukov, H. Hong, and E. Tamer. Estimation and confidence regions for parameter sets in econometric models 1. *Econometrica*, 75(5):1243–1284, 2007.
- A. Cuevas. Set estimation: Another bridge between statistics and geometry. *Bol. Estad. Investig. Oper*, 25(2):71–85, 2009.
- T. K. Dey. *Curve and surface reconstruction: algorithms with mathematical analysis*, volume 23. Cambridge University Press, 2006.
- T. K. Dey and S. Goswami. Provable surface reconstruction from noisy samples. *Computational Geometry*, 35(1-2):124–141, 2006.
- M. Drton and S. Sullivant. Algebraic statistical models. *Statistica Sinica*, pages 1273–1297, 2007.
- B. Efron. Defining the curvature of a statistical problem (with applications to second order efficiency). *The Annals of Statistics*, 3(6):1189–1242, 1975.
- B. Efron. The geometry of exponential families. *The Annals of Statistics*, 6(2):362–376, 1978.
- H. Federer. Curvature measures. *Transactions of the American Mathematical Society*, 93(3):418–491, 1959.
- C. R. Genovese, M. Perone-Pacífico, I. Verdinelli, and L. Wasserman. Nonparametric ridge estimation. *The Annals of Statistics*, 42(4):1511–1545, 2014.
- P. Gibilisco, E. Riccomagno, M. P. Rogantin, and H. P. Wynn. *Algebraic and geometric methods in statistics*. Cambridge University Press, 2010.
- K. Grove and H. Karcher. How to conjugate \mathbb{C} -close group actions. *Mathematische Zeitschrift*, 132(1):11–20, 1973.
- L. P. Hansen. Large sample properties of generalized method of moments estimators. *Econometrica: Journal of the Econometric Society*, pages 1029–1054, 1982.
- L. P. Hansen and K. J. Singleton. Generalized instrumental variables estimation of nonlinear rational expectations models. *Econometrica: Journal of the Econometric Society*, pages 1269–1286, 1982.
- R. A. Horn and C. R. Johnson. *Matrix analysis*. Cambridge university press, 2012.
- M. Irwin. *Smooth dynamical systems*. Academic Press, 1980.
- K. Jisu, Y.-C. Chen, S. Balakrishnan, A. Rinaldo, and L. Wasserman. Statistical inference for cluster trees. In *Advances in Neural Information Processing Systems*, pages 1839–1847, 2016.
- T. Laloe and R. Servien. Nonparametric estimation of regression level sets. *Journal of the Korean Statistical Society*, 2013.
- K.-Y. Liang and S. L. Zeger. Longitudinal data analysis using generalized linear models. *Biometrika*, 73(1):13–22,

- 1986.
- B. G. Lindsay. Mixture models: theory, geometry and applications. In *NSF-CBMS regional conference series in probability and statistics*, pages i–163. JSTOR, 1995.
- E. Mammen and W. Polonik. Confidence regions for level sets. *Journal of Multivariate Analysis*, 122:202–214, 2013.
- C. F. Manski. *Partial identification of probability distributions*. Springer Science & Business Media, 2003.
- P. Mattila. *Geometry of sets and measures in Euclidean spaces: fractals and rectifiability*, volume 44. Cambridge university press, 1999.
- R. McGehee. A stable manifold theorem for degenerate fixed points with applications to celestial mechanics. *Journal of Differential Equations*, 14(1):70–88, 1973.
- R. McGehee and E. Sander. A new proof of the stable manifold theorem. *Zeitschrift für angewandte Mathematik und Physik ZAMP*, 47(4):497–513, 1996.
- M. Michałek, B. Sturmfels, C. Uhler, and P. Zwiernik. Exponential varieties. *Proceedings of the London Mathematical Society*, 112(1):27–56, 2016.
- I. Molchanov. Empirical estimation of distribution quantiles of random closed sets. *Theory of Probability & Its Applications*, 35(3):594–600, 1991.
- I. S. Molchanov. A limit theorem for solutions of inequalities. *Scandinavian Journal of Statistics*, 25(1):235–242, 1998.
- Y. Nesterov. *Lectures on convex optimization*, volume 137. Springer, 2018.
- P. Niyogi, S. Smale, and S. Weinberger. Finding the homology of submanifolds with high confidence from random samples. *Discrete & Computational Geometry*, 39(1-3):419–441, 2008.
- B. Pateiro López. *Set estimation under convexity type restrictions*. Univ Santiago de Compostela, 2008.
- L. Perko. *Differential equations and dynamical systems*, volume 7. Springer Science & Business Media, 2001.
- D. Preiss. Geometry of measures in \mathbb{R}^n : distribution, rectifiability, and densities. *Annals of Mathematics*, 125(3):537–643, 1987.
- W. Qiao and W. Polonik. Nonparametric confidence regions for level sets: Statistical properties and geometry. *Electronic Journal of Statistics*, 13(1):985–1030, 2019.
- W. C. Rheinboldt. On the computation of multi-dimensional solution manifolds of parametrized equations. *Numerische Mathematik*, 1988.
- J. R. Rice. Nonlinear approximation. ii curvature in minkowski geometry and local uniqueness. *Transactions of the American Mathematical Society*, 128(3):437–459, 1967.
- A. Rinaldo and L. Wasserman. Generalized density clustering. *The Annals of Statistics*, 38(5):2678–2722, 2010.
- A. Rinaldo, A. Singh, R. Nugent, and L. Wasserman. Stability of density-based clustering. *The Journal of Machine Learning Research*, 13(1):905–948, 2012.
- J. P. Romano. Bootstrapping the mode. *Annals of the Institute of Statistical Mathematics*, 40(3):565–586, 1988a.
- J. P. Romano. On weak convergence and optimality of kernel density estimates of the mode. *The Annals of Statistics*, pages 629–647, 1988b.
- J. P. Romano and A. M. Shaikh. Inference for the identified set in partially identified econometric models. *Econometrica*, 78(1):169–211, 2010.
- W. Rudin. *Principles of mathematical analysis*, volume 3. McGraw-hill New York, 1964.
- E. Tamer. Partial identification in econometrics. *Annu. Rev. Econ.*, 2(1):167–195, 2010.
- A. B. Tsybakov. On nonparametric estimation of density level sets. *The Annals of Statistics*, 25(3):948–969, 1997.
- A. van der Vaart. *Asymptotic Statistics*. Cambridge University Press, Cambridge, 1998.
- G. Walther. Granulometric smoothing. *The Annals of Statistics*, 25(6):2273–2299, 1997.

APPENDIX B: PROOFS

PROOF OF LEMMA 1. We prove this by showing that any vector v that is perpendicular to the row space of $\nabla\Psi(x)$ must be in the tangent space of M . Let $\Psi(x) = (\Psi_1(x), \dots, \Psi_s(x))$. Any point $x \in M$ satisfies $\Psi_\ell(x) = 0$ for all $\ell = 1, \dots, s$.

It is well known that the gradient vector $\nabla\Psi_\ell(x)$ is perpendicular to the level set $\{z : \Psi_\ell(z) = 0\}$ at x . Thus, the tangent space of the level set $\{z : \Psi_\ell(z) = 0\}$ will be perpendicular to $\nabla\Psi_\ell(x)$ for any $\ell = 1, \dots, s$. Since M can be written as the intersection $\bigcap_{\ell=1}^s \{z : \Psi_\ell(z) = 0\}$, the tangent space of M at x will be the intersection of the tangent spaces of each $\{z : \Psi_\ell(z) = 0\}$ at x . As a result, the normal space will be spanned by $\{\nabla\Psi_\ell(x) : \ell = 1, \dots, s\}$, which proves this lemma.

□

PROOF OF LEMMA 2. Essentially, we only need to show that when $d(x, M) \leq \frac{3\lambda_M^2}{8\|\Psi\|_{\infty,1}^*\|\Psi\|_{\infty,2}^*}$, the minimal eigenvalue $\lambda_{\min}(G_{\Psi}(x)G_{\Psi}(x)^T) \geq \frac{1}{4}\lambda_M^2$.

For any point x with $d(x, M) \leq \frac{3\lambda_M^2}{8\|\Psi\|_{\infty,1}^*\|\Psi\|_{\infty,2}^*}$, let x_M be the projection on M . The minimal eigenvalue

$$(12) \quad \begin{aligned} \lambda_{\min}(G_{\Psi}(x)G_{\Psi}(x)^T) &= \lambda_{\min}(G_{\Psi}(x_M)G_{\Psi}(x_M)^T) \\ &\quad + (\lambda_{\min}(G_{\Psi}(x)G_{\Psi}(x)^T) - \lambda_{\min}(G_{\Psi}(x_M)G_{\Psi}(x_M)^T)) \\ &\geq \lambda_M^2 - |\lambda_{\min}(G_{\Psi}(x)G_{\Psi}(x)^T) - \lambda_{\min}(G_{\Psi}(x_M)G_{\Psi}(x_M)^T)|. \end{aligned}$$

The Weyl's theorem (see, e.g., Theorem 4.3.1 of [Horn and Johnson 2012](#)) shows that the eigenvalue difference can be bounded via

$$\begin{aligned} &|\lambda_{\min}(G_{\Psi}(x)G_{\Psi}(x)^T) - \lambda_{\min}(G_{\Psi}(x_M)G_{\Psi}(x_M)^T)| \\ &\leq \|G_{\Psi}(x)G_{\Psi}(x)^T - G_{\Psi}(x_M)G_{\Psi}(x_M)^T\|_{\max} \\ &\leq 2\|\Psi\|_{\infty,1}^*\|\Psi\|_{\infty,2}^*\|x - x_M\| \quad (\text{by Taylor's theorem}) \\ &= 2\|\Psi\|_{\infty,1}^*\|\Psi\|_{\infty,2}^*d(x, M). \end{aligned}$$

Thus, as long as

$$2\|\Psi\|_{\infty,1}^*\|\Psi\|_{\infty,2}^*d(x, M) \leq \frac{3}{4}\lambda_M^2$$

we have $\lambda_{\min}(G_{\Psi}(x)G_{\Psi}(x)^T) \geq \frac{1}{4}\lambda_M^2$, which completes the proof.

□

PROOF OF THEOREM 3. The proof is modified from the proof of Lemma 4.11 and Theorem 4.12 in [Federer \(1959\)](#).

Let $r_0 = \min\{\frac{\delta_0}{2}, \frac{\lambda_0}{\|\Psi\|_{\infty,2}^*}\}$. We will show that r_0 is a lower bound of $\text{reach}(M)$. We proceed by the proof of contradiction.

Suppose that the conclusion is incorrect that the reach is less than r_0 . Then there exists a point x such that $d(x, M) < r_0$ and x has two projections onto M , denoted as $b, c \in M$.

Since $b, c \in M$, $\Psi(b) = \Psi(c) = 0$ and by Taylor's remainder theorem and condition (F1),

$$(13) \quad \begin{aligned} \|G_{\Psi}(b)(b - c)\|_2 &= \|f(b) - f(c) - G_{\Psi}(b)(b - c)\|_2 \\ &\leq \frac{1}{2}\|b - c\|_2^2\|\Psi\|_{\infty,2}^*. \end{aligned}$$

By the nature of projection, we can find a vector $t_b \in \mathbb{R}^s$ such that $x - b = t_b^T G_{\Psi}(b)$ because the normal space is spanned by the row space of $G_{\Psi}(b)$ (Lemma 1). Together with (13), this implies

$$(14) \quad \begin{aligned} 2|(x - b)^T(b - c)| &= 2|t_b^T G_{\Psi}(b)(b - c)| \\ &\leq \|G_{\Psi}(b)(b - c)\|_2 \|t_b\|_2 \\ &\leq \|\Psi\|_{\infty,2}^*\|b - c\|_2^2 \|t_b\|_2. \end{aligned}$$

such that

$$(21) \quad \phi_x(0) = x, \quad \frac{\partial}{\partial t} \phi_x(t) = -\nabla h(\phi(t)).$$

Later we will prove in Theorem 6 that $\phi_x(\infty) \in M$ when $x \in M \oplus \delta_0$, where δ_0 is defined in Theorem 6.

By Theorem 3.39 in Irwin (1980), $\phi_x(t)$ is uniquely defined since the gradient $\nabla h(x)$ is well-defined for all $x \notin M$. We define an arc-length flow (i.e., a constant velocity flow) based on ϕ_x :

$$(22) \quad \gamma_x(0) = x, \quad \frac{\partial}{\partial t} \gamma_x(t) = -\frac{\nabla h(\gamma_x(t))}{\|\nabla h(\gamma_x(t))\|_2}.$$

The time traveled in this flow is the same as the distance traveled (due to the velocity being a unit vector). Let $T_x = \inf\{t > 0 : \gamma_x(t) \in M\}$ be the terminal time point and let $\gamma_x(T_x) \in M$ as the endpoint of the flow. This means that T_x is the length of the flow from x to the destination on M . The goal is to bound T_x since the length must be greater or equal to the projection distance for $x \in \widetilde{M}$. Note that when $\|\widetilde{\Psi} - \Psi\|_\infty^* \rightarrow 0$, every $x \in \widetilde{M}$ must satisfy $d(x, M) \leq \delta_0$ so that $\phi_x(\infty) \in M$ by Theorem 6.

We define $\xi_x(t) = h(\gamma_x(t)) - h(\gamma_x(T_x)) = h(\gamma_x(t))$. Differentiating $\xi_x(t)$ with respect to t leads to

$$(23) \quad \begin{aligned} \xi_x'(t) &= -\frac{d}{dt} h(\gamma_x(t)) \\ &= -[\nabla h(\gamma_x(t))]^T \frac{d}{dt} \gamma_x(t) \\ &= -\|\nabla h(\gamma_x(t))\| \\ &= -\frac{\|\Psi(\gamma_x(t))^T G_\Psi(\gamma_x(t))\|_2}{\|\Psi(\gamma_x(t))\|_2} \\ &\leq -\lambda_{\min}(G_\Psi(\gamma_x(t))G_\Psi(\gamma_x(t))^T) \\ &\leq -\lambda_0 \end{aligned}$$

because $\gamma_x(t) \in M \oplus \delta_0$ for all t .

Let $\epsilon_0 = \|\Psi - \widetilde{\Psi}\|_{\infty,0}^* = \sup_x \|\Psi(x) - \widetilde{\Psi}(x)\|_{\max}$ and recall that $x \in \widetilde{M}$ so $\widetilde{\Psi}(x) = 0$. Then by the fact that $\|v\|_2 \leq \sqrt{d} \times \|v\|_{\max}$ for vector v ,

$$\begin{aligned} \sqrt{d} \cdot \epsilon_0 &= \sqrt{d} \sup_x \|\Psi(x) - \widetilde{\Psi}(x)\|_{\max} \\ &\geq \sup_x \|\Psi(x) - \widetilde{\Psi}(x)\| \\ &\geq \|\Psi(x) - \widetilde{\Psi}(x)\| \\ &\geq h(x) \\ &= h(\gamma_x(0)) - h(\gamma_x(T_x)) \quad (\text{since } h(\gamma_x(T_x)) = 0) \\ &= \xi(0) - \xi(T_x) \quad (\xi(T_x) = 0 \text{ and } \xi(0) = h(0)) \\ &= -T_x \xi'(T_x^*) \quad (\text{mean value Theorem}) \\ &\geq T_x \lambda_0 \quad \text{by equation (23)}. \end{aligned}$$

Hence, $T_x \leq \frac{\sqrt{d}}{\lambda_0} \epsilon_0 = O(\epsilon_0)$ which is independent of x . This implies that

$$\sup_{x \in \widetilde{M}} d(x, M) \leq \frac{\sqrt{d}}{\lambda_0} \epsilon_0.$$

Similarly, we can exchange \widetilde{M} and M and repeat the above proof, which leads to

$$\sup_{x \in M} d(x, \widetilde{M}) \leq \frac{\sqrt{d}}{\lambda_0} \epsilon_0.$$

As a result, we conclude that $\text{Haus}(\widetilde{M}, M) \leq \frac{\sqrt{d}}{\lambda_0} \epsilon_0 = O(\epsilon_0)$.

3. By Theorem 3, the reach of M has lower bound $\min\{\delta_0/2, \lambda_0/\|\Psi\|_{\infty,2}^*\}$. Note that δ_0, λ_0 depends on the first derivative of Ψ . Hence, the lower bound for reach of M and \widetilde{M} will be bounded at rate $O(\|\Psi - \widetilde{\Psi}\|_{\infty,2}^*)$.

□

Before moving forward, we would like to note that the gradient and Hessian of f can be expressed as

$$(24) \quad G_f(x) = \nabla f(x) = 2\Psi(x)^T \Lambda [\nabla \Psi(x)]$$

$$(25) \quad H_f(x) = \nabla \nabla f(x) = 2[\nabla \Psi(x)]^T \Lambda [\nabla \Psi(x)] + 2\Psi(x) \Lambda [\nabla \nabla \Psi(x)],$$

$$(26) \quad \nabla \nabla \nabla f(x) = 6[\nabla \Psi(x)]^T \Lambda [\nabla \nabla \Psi(x)] + 2\Psi(x) \Lambda [\nabla \nabla \nabla \Psi(x)],$$

where $\nabla \Psi(x) \in \mathbb{R}^{s \times d}$ and $\nabla \nabla \Psi(x) \in \mathbb{R}^{s \times d \times d}$.

PROOF OF LEMMA 5.

Property 1 (For each $x \in M$).

1-(a). By equation (25) and the fact that $\Psi(x) = 0$ whenever $x \in M$, we obtain

$$H_f(x) = 2[\nabla \Psi(x)]^T \Lambda [\nabla \Psi(x)].$$

Because Λ is positive definite, it can be decomposed into $\Lambda = UDU^T$ where D is a diagonal matrix so the eigenvectors corresponding to non-zero eigenvalues of H_f will be the the rows of $U^T [\nabla \Psi(x)]$, which spans the same subspace as the row space of $[\nabla \Psi(x)]$ so by Lemma 1, the non-zero eigenvectors spans the normal space of M at x .

1-(b). Because $H_f(x) = 2[\nabla \Psi(x)]^T \Lambda [\nabla \Psi(x)]$ when $x \in M$, the minimal non-zero eigenvalue

$$\lambda_{\min, >0}(H_f(x)) = 2\lambda_{\min, >0}(G_\Psi(x)^T \Lambda G_\Psi(x)).$$

Since Λ is positive definite and symmetric, we can decompose

$$G_\Psi(x)^T \Lambda G_\Psi(x) = G_\Psi(x)^T \Lambda^{1/2} \Lambda^{1/2} G_\Psi(x)$$

so we obtain

$$\begin{aligned} \lambda_{\min, >0}(H_f(x)) &= 2\lambda_{\min, >0}(G_\Psi(x)^T \Lambda G_\Psi(x)) \\ &= 2\lambda_{\min}(\Lambda^{1/2} G_\Psi(x) G_\Psi(x)^T \Lambda^{1/2}) \\ &\geq 2\Lambda_{\min} \lambda_{\min}(G_\Psi(x) G_\Psi(x)^T) \\ &\geq 2\Lambda_{\min} \lambda_0^2. \end{aligned}$$

1-(c). Because the normal space of M at x is spanned by the rows of $G_\Psi(x) = \nabla\Psi(x)$, which by 1-(a) is spanned by the non-zero eigenvectors of $H_f(x)$, the result follows.

Property 2. Because $d(x, M) < \delta_c$ so x is within the reach of M and thus, x_M , the projection from x onto M , is unique. As a result, the normal space of x_M , $N_M(x)$, is well-defined.

We can decompose

$$\begin{aligned}
\lambda_{\min, \perp, M}(H_f(x)) &= \min_{v \in N_M(x)} \frac{v^T H_f(x) v}{\|v\|^2} \\
&= \min_{v \in N_M(x)} \frac{v^T (H_f(x_M) + H_f(x) - H_f(x_M)) v}{\|v\|^2} \\
&\geq \min_{v \in N_M(x)} \frac{v^T H_f(x_M) v}{\|v\|^2} - \max_{v \in N_M(x)} \frac{v^T (H_f(x) - H_f(x_M)) v}{\|v\|^2} \\
&\geq \min_{v \in N_M(x)} \frac{v^T H_f(x_M) v}{\|v\|^2} - d \|H_f(x) - H_f(x_M)\|_{\max} \\
&\geq 2\lambda_0^2 \Lambda_{\min} - d \|H_f(x) - H_f(x_M)\|_{\max}
\end{aligned}$$

By equation (25),

$$\begin{aligned}
\|H_f(x) - H_f(x_M)\|_{\max} &\leq 2 \|G_\Psi(x)^T \Lambda G_\Psi(x) - G_\Psi(x_M)^T \Lambda G_\Psi(x_M)\|_{\max} \\
&\quad + 2 \|\Psi(x) \Lambda H_\Psi(x) - \Psi(x_M) \Lambda H_\Psi(x_M)\|_{\max} \\
&\leq 4 \|\Psi\|_{\infty, 1}^* \Lambda_{\max} \|\Psi\|_{\infty, 2}^* \|x - x_M\| + 4 \|\Psi\|_{\infty, 2}^* \Lambda_{\max} \|\Psi\|_{\infty, 3}^* \|x - x_M\| \\
&\leq 8 \|\Psi\|_{\infty, 2}^* \Lambda_{\max} \|\Psi\|_{\infty, 3}^* \|x - x_M\|.
\end{aligned}$$

Thus, as long as

$$\|x - x_M\| = d(x, M) \leq \frac{\lambda_0^2 \Lambda_{\min}}{8d \Lambda_{\max} \|\Psi\|_{\infty, 2}^* \|\Psi\|_{\infty, 3}^*},$$

we have

$$\lambda_{\min, \perp, M}(H_f(x)) \geq \lambda_0^2 \Lambda_{\min},$$

which completes the proof.

□

PROOF OF THEOREM 6.

1. Convergence radius. We prove this by showing that for any $x \in M \oplus \delta_c$, the destination $\pi_x(\infty) \in M$. The idea of the proof relies on two properties:

- (P1) Any stationary point of f inside $M \oplus \delta_c$ must be a point in M .
- (P2) Let x_M be a point on M that is closest to x . For any point $x \in M \oplus \delta_c$, $(x - x_M)^T \nabla f(x) > 0$. Namely, the gradient flow only moves $\pi_x(t)$ closer toward M .

With the above two properties, it is easy to see that if we start a gradient flow π_x from $x \in M \oplus \delta_c$, then by (P2) this flow must stay within $M \oplus \delta_c$. Because stationary points within $M \oplus \delta_c$ are all in M by (P1) and the destination of a gradient flow must be a stationary point, we conclude that $\pi_x(\infty) \in M$, which completes the proof of convergence radius. In what follows, we show the two properties.

Property P1: Any stationary point inside $M \oplus \delta_c$ must be a point in M . Because $\nabla f(x) = \Psi(x)\Lambda G_\Psi(x)$ and Λ is positive definite, there are only two cases that $\nabla f(x) = 0$: 1. $\Psi(x) = 0$ and 2., row space of $G_\Psi(x)$ has a dimension less than s (in fact, if $\Psi(x) \neq 0$, then the second case is a necessary condition). The first case is the solution manifold M so we only need to focus on showing that the second case will not happen for $x \in M \oplus \delta_c$.

The row space of $G_\Psi(x)$ has a dimension less than s when there exists a singular value of $G_\Psi(x)$ being 0; or equivalently, $\lambda_{\min}(G_\Psi(x)G_\Psi(x)^T) = 0$. However, assumption (F2) already requires that this will not happen within $M \oplus \delta_c$. Thus, this property holds.

Property P2: For any $x \in M \oplus \delta_c$, the directional gradient $(x - x_M)^T \nabla f(x) > 0$. By Taylor expansion and property 2 of Lemma 5,

$$\begin{aligned}
(x - x_M)^T \nabla f(x) &= (x - x_M)^T (\nabla f(x) - \underbrace{\nabla f(x_M)}_{=0}) \\
(27) \quad &= (x - x_M)^T \int_{\epsilon=0}^{\epsilon=1} H_f(x_M + \epsilon(x - x_M))(x - x_M) d\epsilon \\
&\geq \|x - x_M\|^2 \inf_{y \in M \oplus \delta_c} \lambda_{\min, \perp, M}(H_f(y)) \\
&\geq d(x, M)^2 \lambda_0^2 \Lambda_{\min} > 0
\end{aligned}$$

2. Terminal flow orientation. To study the gradient flow close to M , it suffices to analyze the behavior of gradient close to M . Let $x \in M$ and define u to be a unit vector in the normal space of M at x . By Lemma 1, u belongs to the row space of $\nabla \Psi(x) = G_\Psi(x)$.

Now we consider the gradient at $x + \epsilon u$ when $\epsilon \rightarrow 0$. By Taylor's theorem and the fact that f has bounded third derivatives,

$$G_f(x + \epsilon u) \equiv \nabla f(x + \epsilon u) = \nabla f(x + \epsilon u) - \nabla f(x) = \epsilon H_f(x)u + O(\epsilon^2).$$

Thus,

$$\lim_{\epsilon \rightarrow 0} \frac{1}{\epsilon} G_f(x + \epsilon u) = H_f(x)u.$$

By equation (25),

$$H_f(x) = 2G_\Psi(x)^T \Lambda G_\Psi(x) + 2\Psi(x)\Lambda H_\Psi(x) = 2G_\Psi(x)^T \Lambda G_\Psi(x)$$

because $\Psi(x) = 0$ when $x \in M$. Using the fact that $G_\Psi(x)^T = [\nabla \Psi_1(x), \dots, \nabla \Psi_s(x)]$, it is easy to see that

$$H_f(x)u = \sum_{\ell=1}^s a_\ell \nabla \Psi_\ell(x),$$

where $a_\ell = e_\ell^T \Lambda G_\Psi(x)u$ with $e_\ell = (0, 0, \dots, 0, 1, 0, \dots, 0)^T \in \mathbb{R}^s$ is the coordinate vector pointing toward ℓ -th coordinate. Thus, by Lemma 1 $\nabla \nabla f(x)u$ belongs to the normal space of M at x , which completes the proof of terminal orientation.

3. Projection. To prove this result, we consider a reparametrization of the gradient flow π_x using a 'unit gradient flow' γ_x similar to equation (22) such that

$$\gamma_x(0) = x, \quad \gamma'_x(t) = \frac{\nabla f(\gamma_x(t))}{\|\nabla f(\gamma_x(t))\|} = \frac{G_f(\gamma_x(t))}{\|G_f(\gamma_x(t))\|}.$$

Using γ_x , the time traveled can be interpreted as distance traveled. Let $T_x = \inf\{t > 0 : \gamma_x(t) \in M\}$ be the time to arrive at M . It is easy to see that when $x \rightarrow M$, $T_x \rightarrow 0$. Define the objective function

along γ_x as $\xi_x(t) = f(\gamma_x(t))$. It is easy to see that $\eta_x(0) = \xi_x(0)$ and $\eta_x(\infty) = \xi_x(T_x) = 0$. The quantity $\xi_x(t)$ has the following properties:

$$\begin{aligned}\xi'_x(t) &= G_f(\gamma_x(t))^T \gamma'_x(t) = \|G_f(\gamma_x(t))\| \\ \xi''_x(t) &= \frac{[\frac{d}{dt}G_f(\gamma(t))]^T G_f(\gamma_x(t))}{\|G_f(\gamma_x(t))\|} \\ &= \frac{G_f(\gamma(t))^T H_f(\gamma(t)) G_f(\gamma(t))}{\|G_f(\gamma_x(t))\|^2} \\ &= \gamma_x(t)^T H_f(\gamma(t)) \gamma_x(t).\end{aligned}$$

Finally, because when $\eta_x(0) = \xi_x(0) \rightarrow 0$, $T_x \rightarrow 0$ so

$$\begin{aligned}\eta_x(0) = \xi_x(0) &= \xi_x(0) - \xi_x(T_x) = \int_{t=0}^{t=T_x} \xi'_x(t) dt \\ &= \int_{t=0}^{t=T_x} (\xi'_x(t) - \xi'_x(T_x)) dt \\ &= \int_{t=0}^{t=T_x} (\xi''_x(T_x)(t - T_x) + O(T_x^2)) dt \\ &= \frac{1}{2} T_x^2 \xi''_x(T_x) + O(T_x^3).\end{aligned}$$

Because $\gamma_x(T_x)$ belongs to the normal space of $H_f(T_x) = \nabla \nabla f(T_x)$, $\xi''_x(t) \geq c_1 > 0$ for some constant c_1 so asymptotically

$$\eta_x(0) \geq c_1 T_x^2 \xi''_x(T_x)$$

which implies $T_x = O(\sqrt{\eta_x(0)})$ and $\|x - \pi_x(\infty)\| \leq T_x = O(\sqrt{\eta_x(0)})$.

□

PROOF OF THEOREM 7.

We prove this result using the idea of the Lyapunov-Perron method (Perko, 2001). Recall that $A(z) = \{x : \pi_x(\infty) = z\}$ for $z \in M$ is the basin of attraction of point z . Consider a ball $B(z, r)$ such that any gradient flow $\pi_x(t)$ that converges to $z = \pi_x(\infty)$ intersects one and only one point at the boundary $\partial B(z, r) = \{y : \|y - z\| = r\}$. This occurs when $r < \delta_c$ due to property (P2) in the proof of Theorem 6.

Consider the gradient flow $\pi_x(t)$ with $x \in \partial B(z, r)$ and $\pi_x(\infty) = z$. By Taylor's theorem, this flow solves the following equation

$$\begin{aligned}(28) \quad \pi'_x(t) &= -G_f(\pi_x(t)) = -G_f(\pi_x(t)) + \underbrace{G_f(\pi_x(\infty))}_{=0} \\ &= -H_f(\pi_x(\infty))(\pi_x(t) - \pi_x(\infty)) + \epsilon(\pi_x(t)),\end{aligned}$$

where $\|\epsilon(\pi_x(t))\| \leq C_0 \|\pi_x(t) - \pi_x(\infty)\| \leq C_0 r$ for some finite constant C_0 due to Assumption (F1). Equation (28) is a perturbed ODE with a fixed point $\pi_x(\infty)$ and by the variation of parameters, its solution can be written as

$$\pi_x(t) - \pi_x(\infty) = e^{-tH_f(\pi_x(\infty))}(\pi_x(0) - \pi_x(\infty)) + \int_{s=0}^{s=t} e^{-(t-s)H_f(\pi_x(\infty))} \epsilon(\pi_x(s)) ds.$$

Denoting $v_x = \pi_x(0) - \pi_x(\infty)$, we can rewrite the flow as

$$\pi_x(t) - \pi_x(\infty) = e^{-tH_f(\pi_x(\infty))}v_x + \int_{s=0}^{s=t} e^{-(t-s)H_f(\pi_x(\infty))}\epsilon(\pi_x(s))ds.$$

By Lemma 1, the normal space of M at $z = \pi_x(\infty)$ is the row space of $G_\Psi(z) = \nabla\Psi(z)$, which will also be the space spanned by the eigenvectors of $H_f(\pi_x(\infty))$ that corresponds to non-zero eigenvalues (Lemma 5 1-(a)). The spectral decomposition shows $H_f(\pi_x(\infty)) = \sum_{\ell=1}^s \lambda_\ell u_\ell u_\ell^T$ and we define the projection matrix onto the normal space of M as $\Pi_N = \sum_{\ell=1}^s u_\ell u_\ell^T$ and the projection matrix onto the tangent space of M as $\Pi_T = I_d - \Pi_N$. By construction, $\Pi_N H_f(\pi_x(\infty)) = H_f(\pi_x(\infty))$ and $\Pi_T H_f(\pi_x(\infty)) = 0$ so $\Pi_N e^{-tH_f(\pi_x(\infty))} = e^{-tH_f(\pi_x(\infty))}$ and $\Pi_T e^{-tH_f(\pi_x(\infty))} = \Pi_T$.

We decompose

$$\begin{aligned} \pi_x(t) - \pi_x(\infty) &= \Pi_T(\pi_x(t) - \pi_x(\infty)) + \Pi_N(\pi_x(t) - \pi_x(\infty)) \\ &= \Pi_T e^{-tH_f(\pi_x(\infty))}v_x + \Pi_T \int_{s=0}^{s=t} e^{-(t-s)H_f(\pi_x(\infty))}\epsilon(\pi_x(s))ds \\ &\quad + \Pi_N e^{-tH_f(\pi_x(\infty))}v_x + \Pi_N \int_{s=0}^{s=t} e^{-(t-s)H_f(\pi_x(\infty))}\epsilon(\pi_x(s))ds \\ (29) \quad &= v_{x,T} + \int_{s=0}^{s=t} \epsilon_T(\pi_x(s))ds + e^{-tH_f(\pi_x(\infty))}v_{x,N} \\ &\quad + \int_{s=0}^{s=t} e^{-(t-s)H_f(\pi_x(\infty))}\epsilon_N(\pi_x(s))ds, \end{aligned}$$

where

$$v_{x,T} = \Pi_T v_x, \quad v_{x,N} = \Pi_N v_x, \quad \epsilon_T(\pi_x(s)) = \Pi_T \epsilon(\pi_x(s)), \quad \epsilon_N(\pi_x(s)) = \Pi_N \epsilon(\pi_x(s)).$$

In the tangent direction, when $t \rightarrow \infty$

$$\begin{aligned} 0 &= \lim_{t \rightarrow \infty} \Pi_T(\pi_x(t) - \pi_x(\infty)) \\ &= \lim_{t \rightarrow \infty} \Pi_T e^{-tH_f(\pi_x(\infty))}v_x + \lim_{t \rightarrow \infty} \Pi_T \int_{s=0}^{s=t} e^{-(t-s)H_f(\pi_x(\infty))}\epsilon(\pi_x(s))ds \\ &= \Pi_T v_x + \int_{s=0}^{s=\infty} \Pi_T \epsilon(\pi_x(s))ds \\ &= v_{x,T} + \int_{s=0}^{s=\infty} \epsilon_T(\pi_x(s))ds. \end{aligned}$$

Thus,

$$(30) \quad v_{x,T} = - \int_{s=0}^{s=\infty} \epsilon_T(\pi_x(s))ds$$

and equation (29) can be rewritten as

$$\begin{aligned} \pi_x(t) - \pi_x(\infty) &= - \int_{s=0}^{s=\infty} \epsilon_T(\pi_x(s))ds + \int_{s=0}^{s=t} \epsilon_T(\pi_x(s))ds \\ &\quad + e^{-tH_f(\pi_x(\infty))}v_{x,N} + \int_{s=0}^{s=t} e^{-(t-s)H_f(\pi_x(\infty))}\epsilon_N(\pi_x(s))ds \\ (31) \quad &= e^{-tH_f(\pi_x(\infty))}v_{x,N} + \int_{s=0}^{s=t} e^{-(t-s)H_f(\pi_x(\infty))}\epsilon_N(\pi_x(s))ds \\ &\quad - \int_{s=t}^{s=\infty} \epsilon_T(\pi_x(s))ds. \end{aligned}$$

The latter two terms involving integral are determined entirely by the Taylor remainder terms $\epsilon(\pi_x(t))$. Thus, to uniquely determine a point on the gradient flow $\pi_x(t)$ that converges to z (and is inside $B(z, r)$), we only need to specify the time t and the vector $v_{x,N}$ that belongs to the normal space of M at z with $\|v_{x,N}\| = r$. Namely, there exists a mapping (due to equation (31)) Ω such that

$$\pi_x(t) = \Omega(t, v_{x,N})$$

for all $\pi_x(t)$ with $\|x - z\| = r$. Note that equation (31) implies that the mapping Ω has bounded derivative with respect to both t and $v_{x,N}$. Therefore, the set

$$A(z) \cap B(z, r) = \left\{ \pi_x(t) = \Omega(t, v_{x,N}) : t \in [0, \infty), v_{x,N} = \sum_{\ell=1}^s a_\ell u_\ell, \sum_{\ell=1}^s a_\ell^2 = r^2 \right\}$$

is parameterized by (t, a_1, \dots, a_s) with a constraint $\sum_{\ell=1}^s a_\ell^2 = r^2$ so it is an s -dimensional manifold.

To generalize this to the entire set $A(z)$, note that every gradient flow ending at z must pass the boundary $\partial B(z, r)$ so allowing the gradient $\pi_x(t)$ to move toward $t \rightarrow -\infty$ covers the entire basin, i.e.,

$$A(z) = \left\{ \pi_x(t) = \Omega(t, v_{x,N}) : t \in \mathbb{R}, v_{x,N} = \sum_{\ell=1}^s a_\ell u_\ell, \sum_{\ell=1}^s a_\ell^2 = r^2 \right\}.$$

This implies that $A(z)$ is parametrized by (t, a_1, \dots, a_s) with a constraint $\sum_{\ell=1}^s a_\ell^2 = r^2$ so again it is an s -dimensional manifold.

□

PROOF OF THEOREM 8.

Convergence of $f(x_t)$. Because $x_{t+1} = x_t - \gamma G_f(x_t)$, simple Taylor expansion shows that

$$\begin{aligned} f(x_t) - f(x_{t+1}) &= f(x_t) - f(x_t - \gamma G_f(x_t)) \\ &= \gamma \|G_f(x_t)\|^2 - \frac{1}{2} \gamma^2 \int_{\epsilon=0}^{\epsilon=1} G_f(x_t) H_f(x_t - \epsilon \gamma G_f(x_t)) G_f(x_t) d\epsilon \\ &\geq \gamma \|G_f(x_t)\|^2 - \frac{1}{2} \gamma^2 \|G_f(x_t)\|^2 \sup_z \|H_f(z)\|_2. \end{aligned}$$

Note that one can also use the fact that the gradient G_f is Lipschitz to obtain a similar bound.

Thus, when $\gamma < \frac{2}{\sup_z \|H_f(z)\|_2}$, we obtain

$$f(x_t) - f(x_{t+1}) > 0$$

which implies that $f(x_{t+1}) < f(x_t)$, i.e., the objective function is decreasing. We can summarize the result as

$$(32) \quad f(x_{t+1}) \leq f(x_t) - \gamma \|G_f(x_t)\|^2 \left(1 - \frac{1}{2} \gamma \sup_z \|H_f(z)\|_2 \right).$$

To obtain the algorithmic convergence rate, we need to associate the objective function $f(x)$ and the squared gradient $\|G_f(x)\|^2$. We focus on the case of $t = 0$, and investigate

$$(33) \quad f(x_1) \leq f(x_0) - \gamma \|G_f(x_0)\|^2 \left(1 - \frac{1}{2} \gamma \sup_z \|H_f(z)\|_2 \right).$$

Because $d(x_0, M) \leq \delta_c \leq \text{reach}(M)$, there is a unique projection $x_M \in M$ from x_0 . Note that $d(x_0, M) = \|x_0 - x_M\|$. The gradient has a lower bound from the following Taylor expansion:

$$\begin{aligned}
\|G_f(x_0)\| &= \|G_f(x_0) - \underbrace{G_f(x_M)}_{=0}\| \\
&= \left\| \int_{\epsilon=0}^{\epsilon=1} H_f(x_M + \epsilon(x_0 - x_M))(x_0 - x_M) d\epsilon \right\| \\
&\geq \|x_0 - x_M\| \inf_{\epsilon \in [0,1]} \lambda_{\min, \perp}(H_f(x_M + \epsilon(x_0 - x_M))) \\
&\geq \|x_0 - x_M\| \lambda_0^2 \Lambda_{\min} \\
&\geq d(x_0, M) \lambda_0^2 \Lambda_{\min},
\end{aligned}$$

where the second to the last inequality is due to property 2 in Lemma 5. Thus,

$$(34) \quad \|G_f(x_0)\|^2 \geq d(x_0, M)^2 \lambda_0^4 \Lambda_{\min}^2.$$

The distance $d(x_0, M)$ and the objective function $f(x_0)$ can also be associated using another Taylor expansion:

$$\begin{aligned}
f(x_0) &= f(x_0) - f(x_M) \\
&= (x_0 - x_M)^T \underbrace{G_f(x_M)}_{=0} + \frac{1}{2} (x_0 - x_M)^T \int_{\epsilon=0}^{\epsilon=1} H_f(x_M + \epsilon(x_0 - x_M)) d\epsilon (x_0 - x_M) \\
&\leq \frac{1}{2} d^2(x_0, M) \sup_z \|H_f(z)\|_2.
\end{aligned}$$

Thus,

$$d^2(x_0, M) \geq \frac{2f(x_0)}{\sup_z \|H_f(z)\|_2}$$

which implies an improved bound on equation (34) as

$$(35) \quad \|G_f(x_0)\|^2 \geq d(x_0, M)^2 \lambda_0^4 \Lambda_{\min}^2 \geq \frac{\lambda_0^4 \Lambda_{\min}^2}{\sup_z \|H_f(z)\|_2} 2f(x_0).$$

By inserting equation (35) into equation (33), we obtain

$$\begin{aligned}
f(x_1) &\leq f(x_0) - \gamma \|G_f(x_0)\|^2 \left(1 - \frac{1}{2} \gamma \sup_z \|H_f(z)\|_2\right) \\
&\leq f(x_0) - \gamma \left(1 - \frac{1}{2} \gamma \sup_z \|H_f(z)\|_2\right) \frac{\lambda_0^4 \Lambda_{\min}^2}{\sup_z \|H_f(z)\|_2} 2f(x_0) \\
&= f(x_0) \left(1 - 2\gamma \left(1 - \frac{1}{2} \gamma \sup_z \|H_f(z)\|_2\right) \frac{\lambda_0^4 \Lambda_{\min}^2}{\sup_z \|H_f(z)\|_2}\right)
\end{aligned}$$

When $\gamma < \frac{1}{\sup_z \|H_f(z)\|_2}$, the above inequality can be simplified as

$$f(x_1) \leq f(x_0) \cdot \left(1 - \gamma \frac{\lambda_0^4 \Lambda_{\min}^2}{\sup_z \|H_f(z)\|_2}\right).$$

Thus, we have proved the result for $t = 0$. The same derivation works for other t (by treating x_t as x_0). By telescoping, we conclude that

$$f(x_t) \leq f(x_0) \cdot \left(1 - \gamma \frac{\lambda_0^4 \Lambda_{\min}^2}{\sup_z \|H_f(z)\|_2}\right)^t.$$

Finally, using the fact that $\sup_z \|H_f(z)\|_2 \leq \Lambda_{\max} \|\Psi\|_{\infty,2}^*$, we obtain the desired bound.

Convergence of $d(x_t, M)$. Let $x_{t,M} \in M$ be the point on the manifold that is closest to x_t ; again, due to the reach condition this projection is unique. The Taylor expansion along with property 2 in Lemma 5 shows that

$$\begin{aligned} -f(x_t) &= f(x_{t,M}) - f(x_t) \\ &= (x_{t,M} - x_t)^T G_f(x_t) + \frac{1}{2} (x_{t,M} - x_t)^T \int_{\epsilon=0}^{\epsilon=1} H_f(x_t + \epsilon(x_{t,M} - x_t)) (x_t - x_{t,M}) d\epsilon \\ &\geq (x_{t,M} - x_t)^T G_f(x_t) + \frac{1}{2} \|x_t - x_{t,M}\|^2 \lambda_0^2 \Lambda_{\min}. \end{aligned}$$

Thus,

$$(36) \quad -f(x_t) - \frac{1}{2} \|x_{t,M} - x_t\|^2 \lambda_0^2 \Lambda_{\min} \geq -(x_t - x_{t,M})^T G_f(x_t).$$

Because of equation (32) and that $\sup_z \|H_f(z)\|_2 \leq d \|\Psi\|_{\infty,2}^*$, we have

$$f\left(x - \frac{1}{d \Lambda_{\max} \|\Psi\|_{\infty,2}^*} G_f(x)\right) - f(x) \leq -\frac{1}{2d \Lambda_{\max} \|\Psi\|_{\infty,2}^*} \|G_f(x)\|^2.$$

Using the fact that $f\left(x - \frac{1}{d \Lambda_{\max} \|\Psi\|_{\infty,2}^*} G_f(x)\right) \geq 0$, we conclude that

$$\frac{1}{2d \Lambda_{\max} \|\Psi\|_{\infty,2}^*} \|G_f(x)\|^2 \leq f(x),$$

which implies

$$(37) \quad \|G_f(x)\|^2 \leq 2d \Lambda_{\max} \|\Psi\|_{\infty,2}^* f(x).$$

For any t , we have

$$\begin{aligned} d(x_{t+1}, M)^2 &\leq \|x_{t+1} - x_{t,M}\|^2 \\ &= \|x_t - x_{t,M} - \gamma G_f(x_t)\|^2 \\ &= \|x_t - x_{t,M}\|^2 - 2(x_t - x_{t,M})^T G_f(x_t) + \gamma^2 \|G_f(x_t)\|^2 \\ &\stackrel{(36)}{\leq} \|x_t - x_{t,M}\|^2 (1 - \gamma \lambda_0^2 \Lambda_{\min}) - 2\gamma f(x_t) + \gamma^2 \|G_f(x_t)\|^2 \\ &\stackrel{(37)}{\leq} \|x_t - x_{t,M}\|^2 (1 - \gamma \lambda_0^2 \Lambda_{\min}) - \underbrace{2\gamma f(x_t) (1 - d\gamma \Lambda_{\max} \|\Psi\|_{\infty,2}^*)}_{\geq 0} \\ &\leq \|x_t - x_{t,M}\|^2 (1 - \gamma \lambda_0^2 \Lambda_{\min}) \\ &= d(x_t, M)^2 (1 - \gamma \lambda_0^2 \Lambda_{\min}) \end{aligned}$$

whenever $\gamma < \frac{1}{\Lambda_{\max} \|\Psi\|_{\infty,2}^*}$. By telescoping, the result follows.
 \square

DEPARTMENT OF STATISTICS
UNIVERSITY OF WASHINGTON
BOX 354322
SEATTLE, WA 98195
E-MAIL: yenchic@uw.edu